11.3 –
Response of Uncontrolled/Controlled Systems in Macro- and Micro-mechanics

Giuseppe Rega

Department of Structural and Geotechnical Engineering
Sapienza University of Rome, Italy
Giuseppe.Rega@uniroma1.it

Coworkers: S. Lenci, P. Goncalves, M. Younis, L. Ruzziconi, D. Orlando, F. Silva

DAY	TIME	LECTURE
Monday 05/11	14.00 -14.45	Historical Framework - A Global Dynamics Perspective in the Nonlinear Analysi of Systems/Structures
	15.00 -15.45	Achieving Load Carrying Capacity: Theoretical and Practical Stability
	16.00 -16.45	Dynamical Integrity: Concepts and Tools_1
Wednesday 07/11	14.00 -14.45	Dynamical Integrity: Concepts and Tools_2
	15.00 -15.45	Global Dynamics of Engineering Systems
	16.00 -16.45	Dynamical integrity: Interpreting/Predicting Experimental Response
Monday 12/11	14.00 -14.45	Techniques for Control of Chaos
	15.00 -15.45	A Unified Framework for Controlling Global Dynamics
	16.00 -16.45	**Response of Uncontrolled/Controlled Systems in Macro- and Micro-mechanic**
Wednesday 14/11	14.00 -14.45	A Noncontact AFM: (a) Nonlinear Dynamics and Feedback Control (b) Global Effects of a Locally-tailored Control
	15.00 -15.45	Exploiting Global Dynamics to Control AFM Robustness
	16.00 -16.45	Dynamical Integrity as a Novel Paradigm for Safe/Aware Design

Overall aims

Investigating the dynamical integrity of different nonlinear mechanical oscillators

- showing practical examples of erosion profiles
- discussing specific mechanical issues
- discussing dynamical issues

different systems ⇨ different dynamical phenomena

- safe basin of steady dynamics always used

Mechanical and dynamical issues

- hardening (Duffing) vs softening (Helmholtz, rigid block, MEMS) systems
- symmetric (Duffing, rigid block) vs asymmetric (Helmholtz, MEMS) systems
- smooth (Helmholtz, Duffing, MEMS) vs non-smooth (rigid block) systems
- various “failure” phenomena: capsizing (Helmholtz), overturning (rigid block), pull-in (MEMS)
- erosion of system without (rigid block) and with (Helmholtz, Duffing, MEMS) internal frequency
- GIM vs IF (rigid block, MEMS)
- harmonic and other excitations

Contents

1. **Integrity of in-well dynamics** (Helmholtz, Duffing, Rigid block, MEMS, Augusti's model, Guyed Tower) → dynamical integrity and control

2. Robustness/Integrity of competing (in-in/in-out) attractors (Duffing, Parametrically excited pendulum, Parametrically excited cylindrical shell)

Helmholtz oscillator

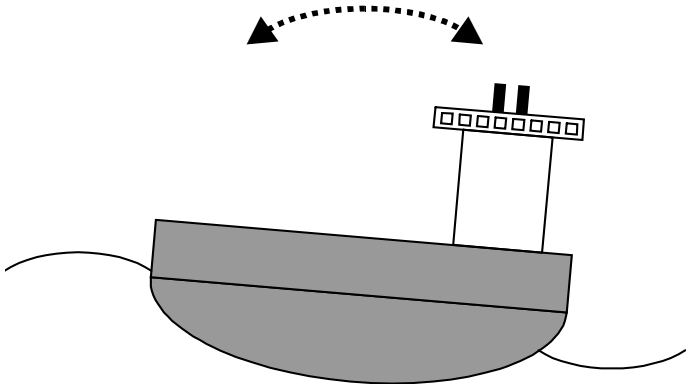

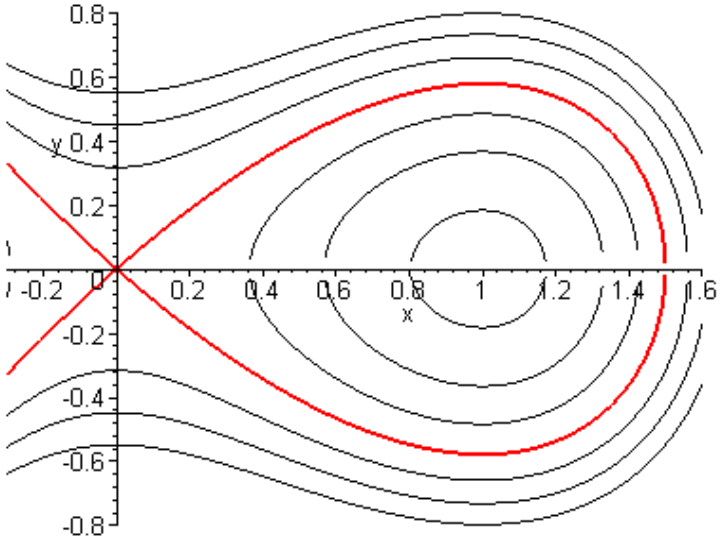

$$\ddot{x}+0.1\dot{x}-x+x^2=\gamma(\omega t)=\gamma_1\sum_{j=1}^{\infty}\frac{\gamma_j}{\gamma_1}\sin(\,j\omega t+\Psi_j)$$

$\varepsilon\gamma_1$ = overall excitation amplitude

γ_j/γ_1; Ψ_j = parameters governing the shape of the excitation

Helmholtz

harmonic

harmonic + 1 super.

harmonic + 2 super.

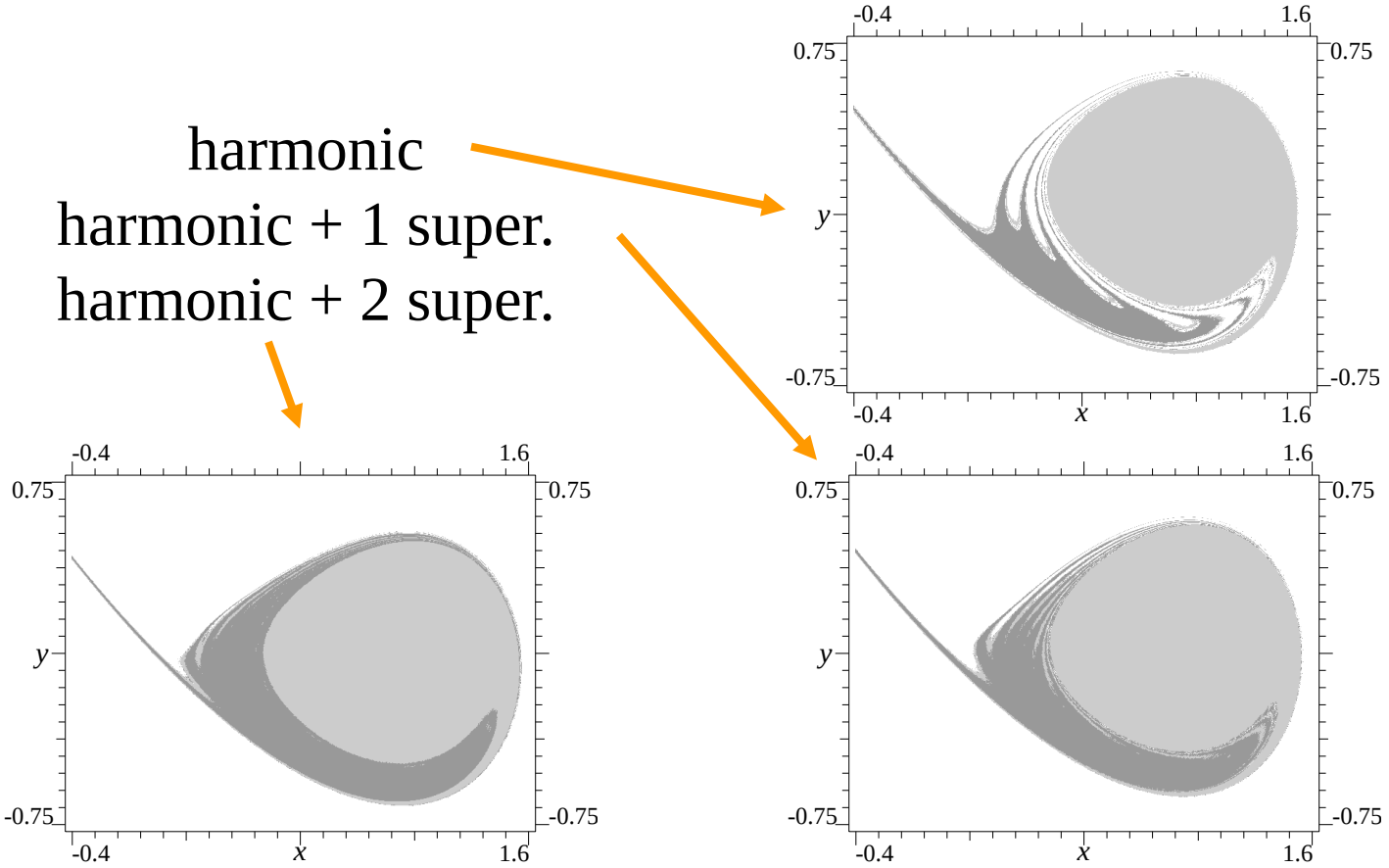

regularization by adding (clever) superharmonics

Helmholtz

higher excitation amplitude

harmonic

harmonic + 1 super.

harmonic + 2 super.

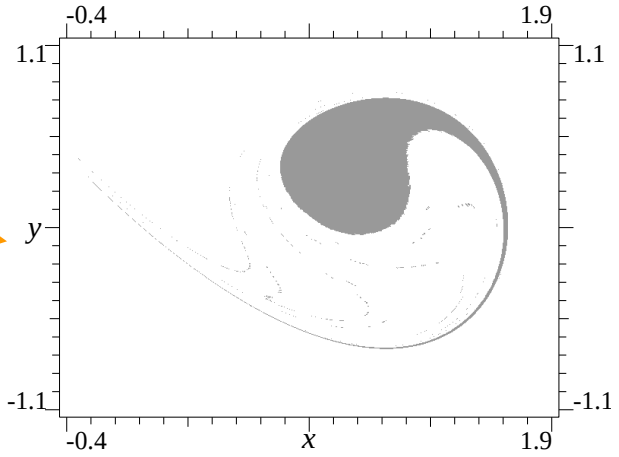

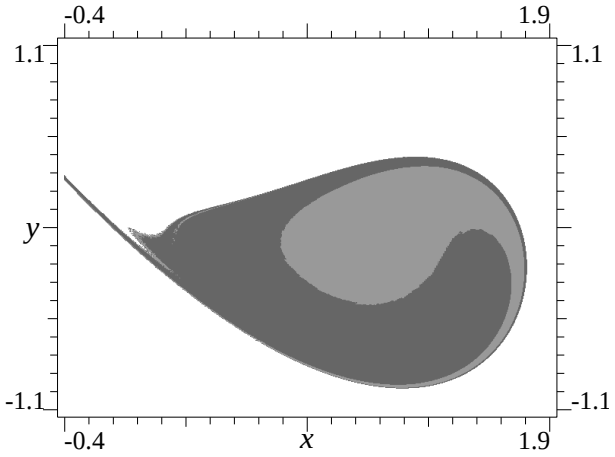

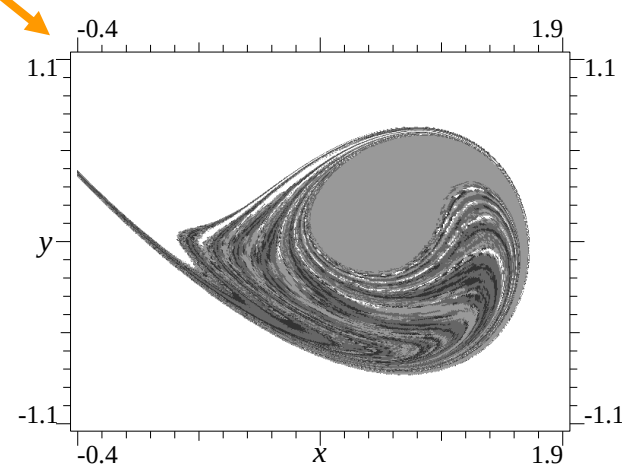

strong reduction for fixed excitation amplitude

Helmholtz: erosion profiles

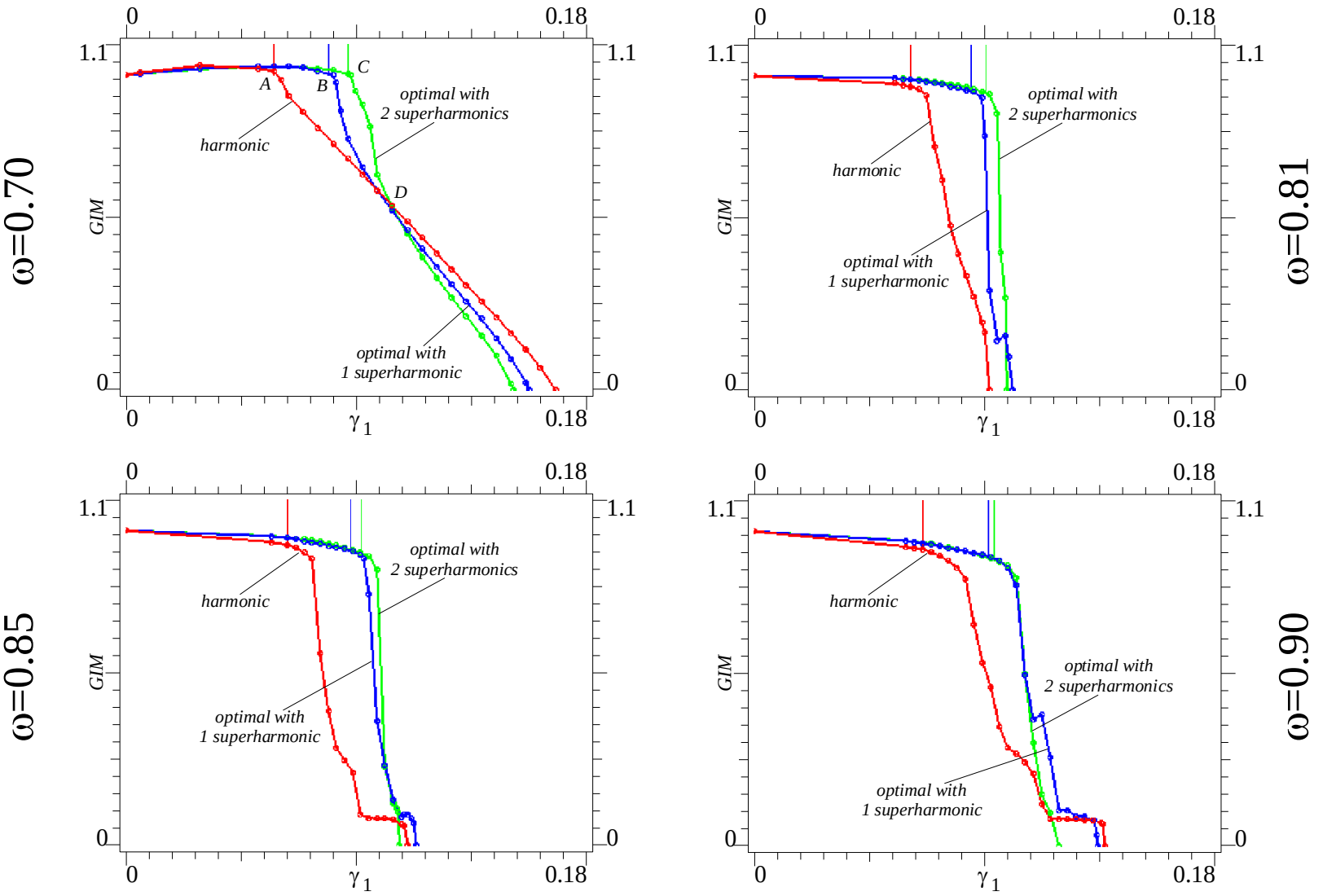

- safe basin: classical basin of attraction; integrity through GIM
- ω=0.81 is the vertex of the escape V-region in parameter plane

Helmholtz: excitation phase-amplitude chart

contour plot of the GIM with harmonic excitation

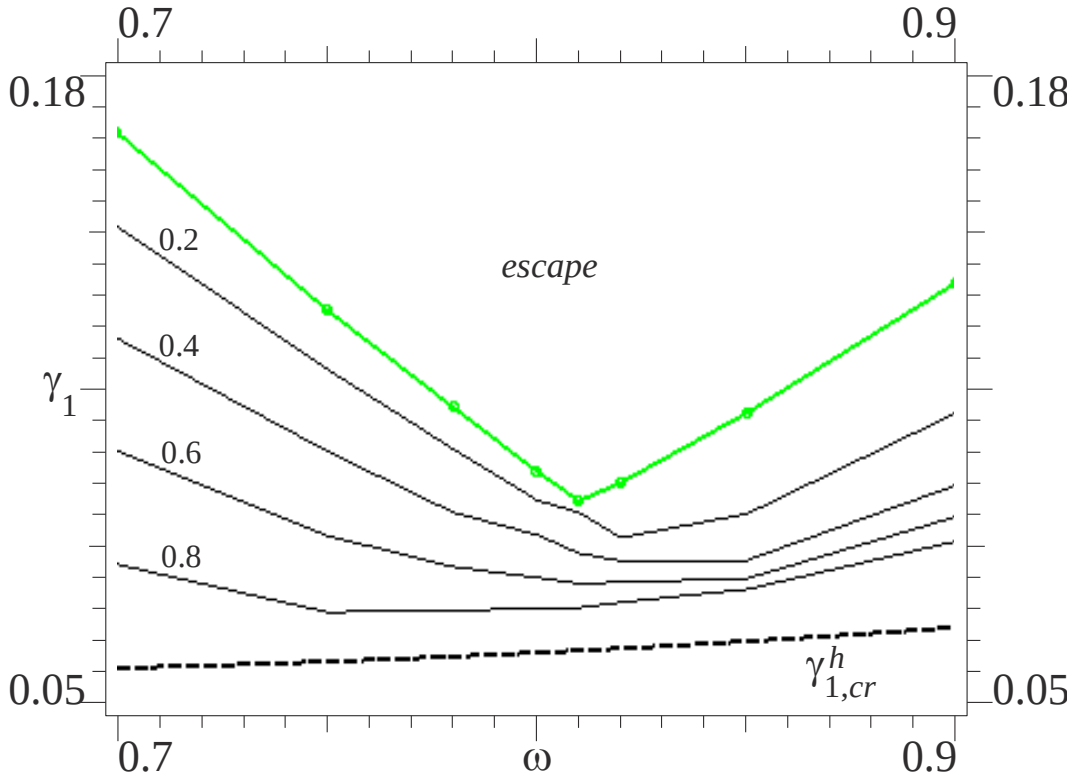

- "Dover cliff" profiles
- starting points of erosion = homoclinic bifurcations (OK!)
- sharpness close to the vertex, dullness elsewhere

Duffing oscillator

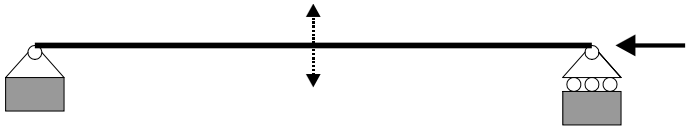

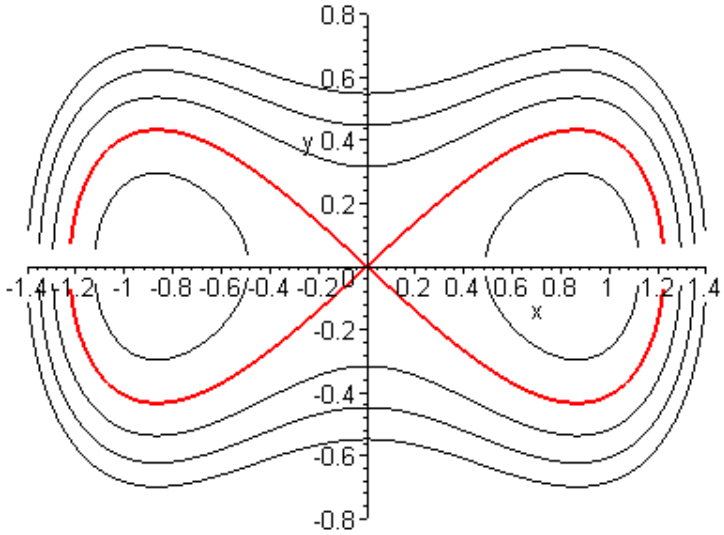

$$\ddot{x} + \varepsilon\delta\dot{x} - \frac{x}{2} + \frac{x^3}{2} = \varepsilon\gamma(\omega t) = \varepsilon\gamma_1 \sum_{j=1}^{\infty} \frac{\gamma_j}{\gamma_1} \sin(j\omega t + \Psi_j)$$

$\varepsilon\gamma_1$= overall excitation amplitude

γ_j/γ_1; Ψ_j= parameters governing the shape of the excitation

Duffing

harmonic

harmonic + 1 sym. super.

harmonic + 1 unsym. super.

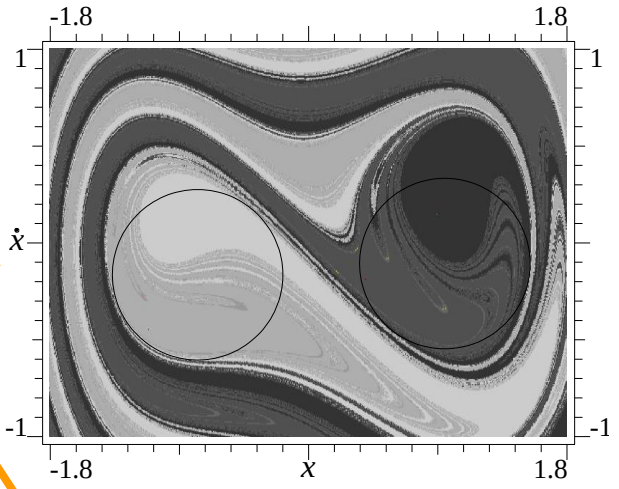

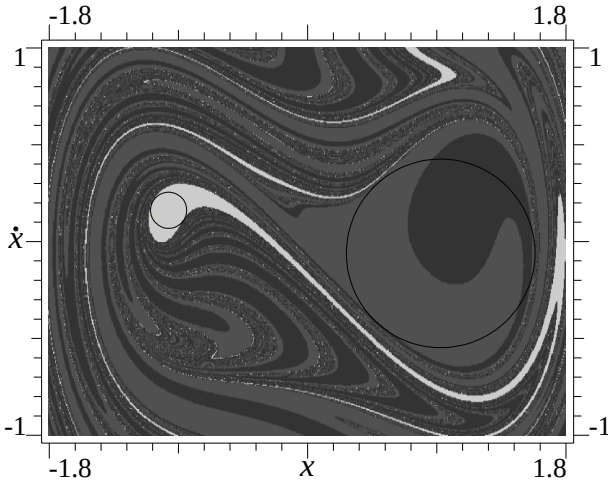

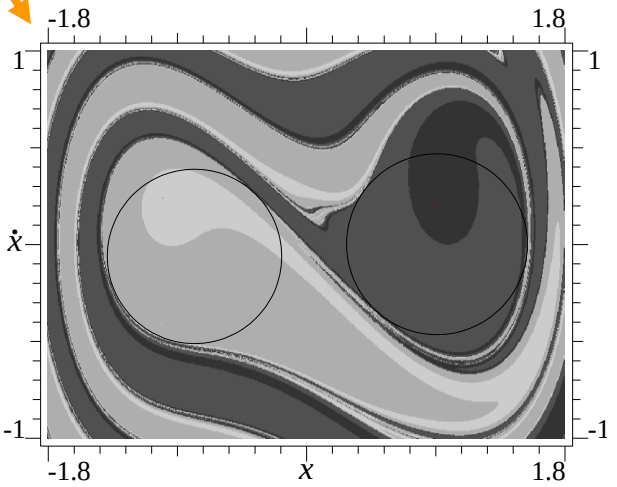

localized vs scattered reduction of fractality

Duffing: erosion profiles

(a) harmonic, (b) harmonic + 1 sym. super.,
(c) harmonic + 1 unsym. super. (in the two different wells)

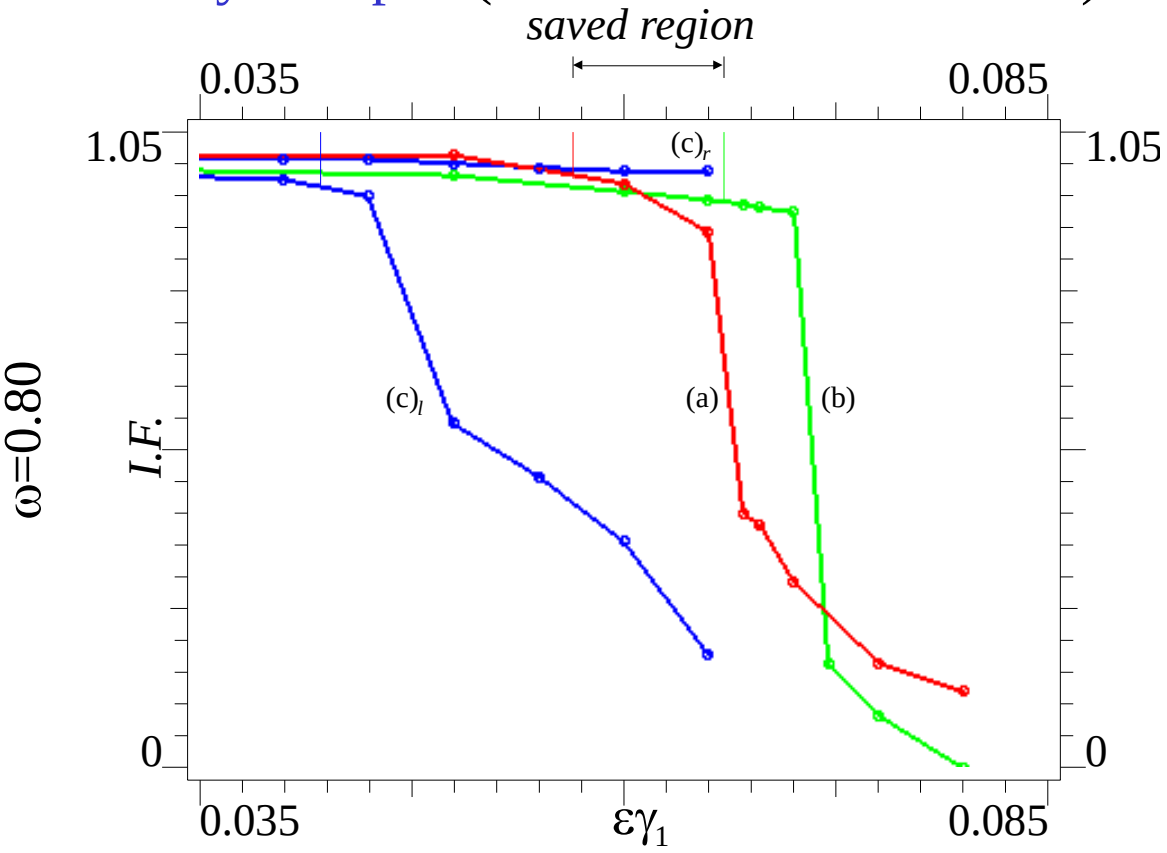

- safe basin: classical basin of attraction; integrity through IF
- ω=0.80 is very close to the vertex of the escape V-region

Rigid block

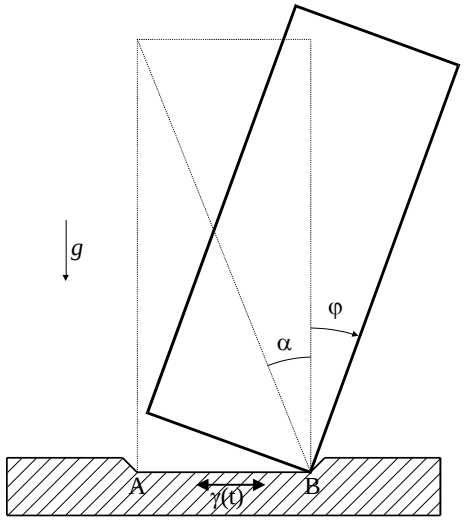

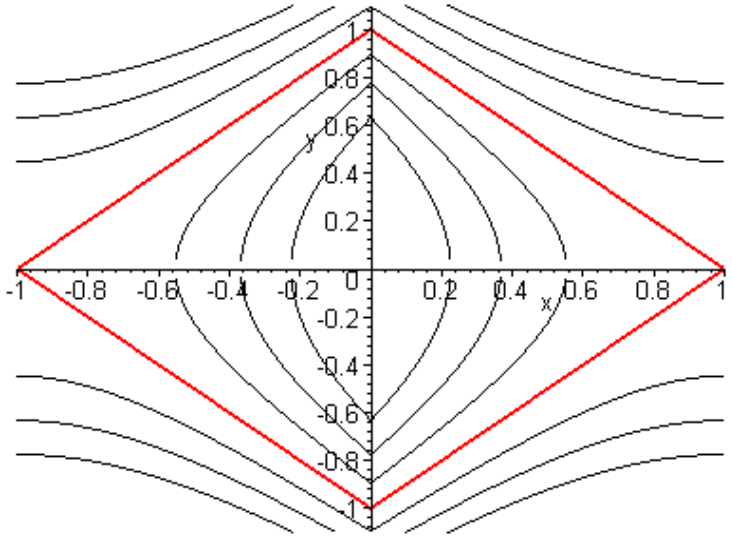

Heteroclinic bifurcation

rocking around the left corner:

$$\ddot{\varphi}+\delta\dot{\varphi}-\varphi-\alpha+\gamma(t)=0, \quad \varphi<0,$$

rocking around the right corner:

$$\ddot{\varphi}+\delta\dot{\varphi}-\varphi+\alpha+\gamma(t)=0, \quad \varphi>0,$$

impact (Newton law):

$$\dot{\varphi}(t^{+})=r\,\dot{\varphi}(t^{-}), \quad \varphi=0,$$

T=2p/w-periodic generic excitation:

$$\gamma(t)=\Sigma_j\,\gamma_j\cos(j\omega t+\psi_j)$$

overturned positions $\varphi=\pm\pi/2$

Rigid block: erosion profiles, different measures

α=0.2, δ=0.02, r=0.95, ω=3.5 (slightly damped) – harmonic excitation

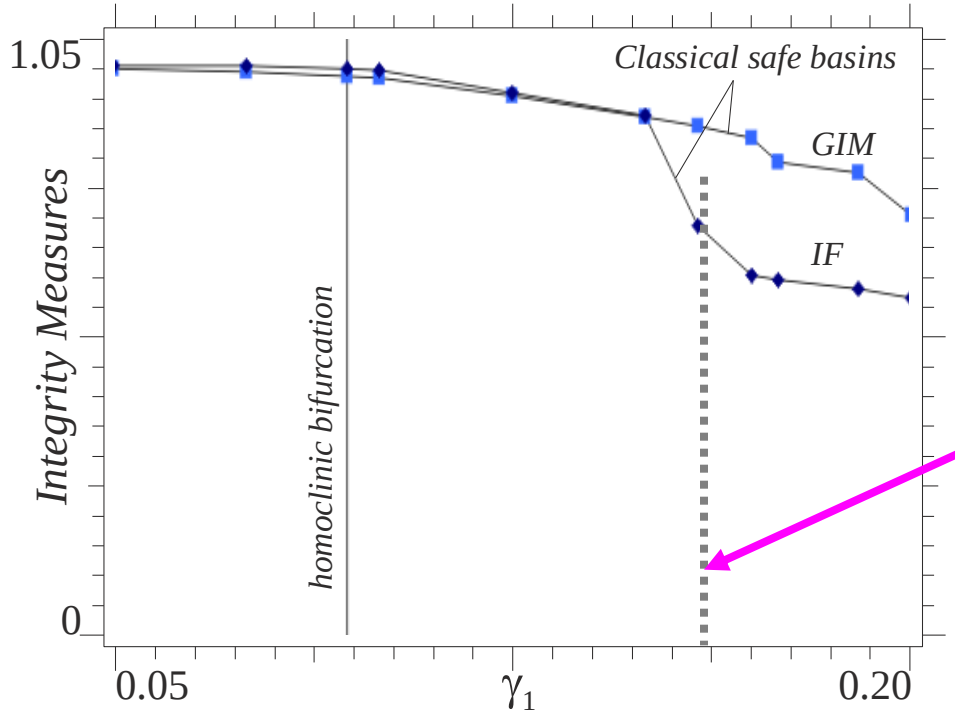

- no resonance frequency around which focusing numerical analyses
- likely effect of a secondary global bifurcation

- GIM misses sharp fall of erosion profile
- high values after fall: absence of resonance?
- homoclinic bifurcation slowly triggers erosion
- effects of non-smoothness

Rigid block: example of basins erosion

γ_1**=0.20** α=0.2, δ=0.5, r=0.7, ω=1.5 γ_1**=0.35**

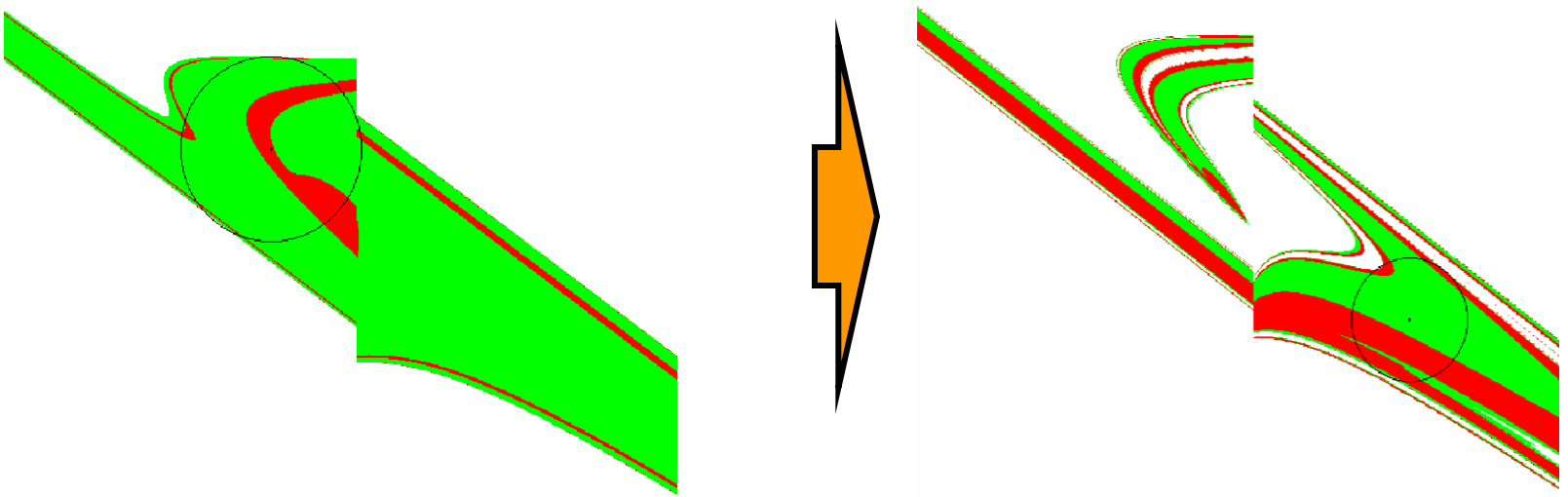

Rigid block: erosion with different excitations

α=0.2, δ=0.5, r=0.7, ω=1.5 (strongly damped)

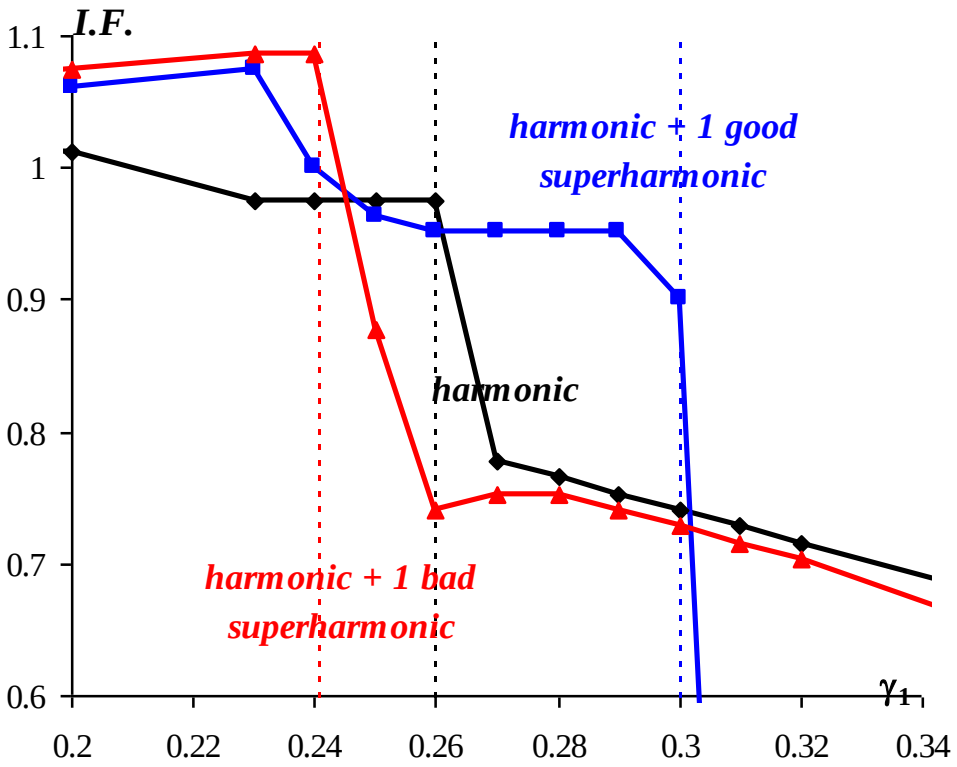

Micro-electro-mechanical systems (MEMS)

- nonlinear dynamics of a thermoelastic microbeam
- axial load, modeling residual stresses

- concentrated electrodynamic transverse force applied at mid-span (the actuation)
- both ends are fixed

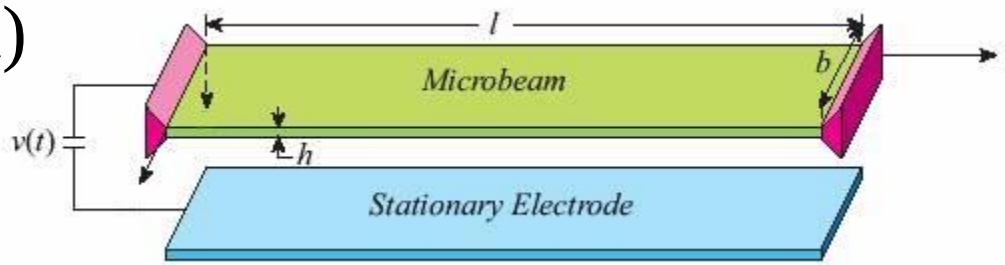

- geometric nonlinearity due to membrane stiffness
- ultra-high vacuum environment

MEMS: single-d.o.f. model

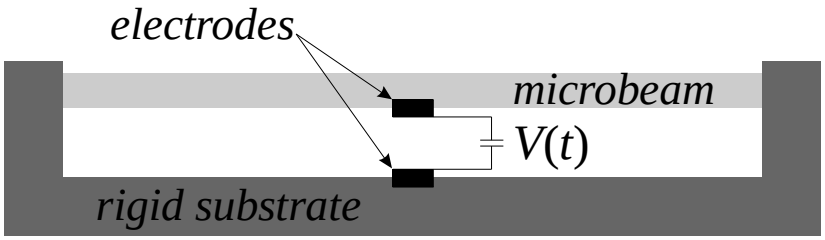

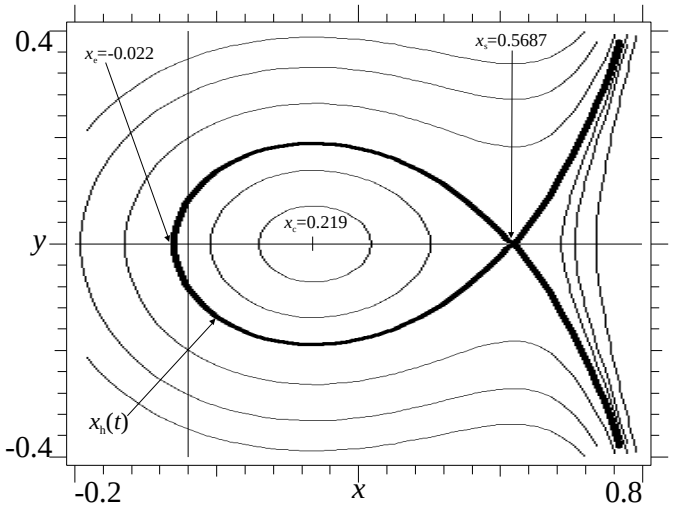

- small electrodynamic force
- small visco- and thermo-elastic damping

→ temperature condensation

$$\ddot{x} + \alpha x + \beta x^3 - \frac{\gamma}{(1-x)^2} = \varepsilon \left\{ -\tilde{\mu}\dot{x} + \frac{\tilde{\eta}\sum_{j=1}^{N} (\eta_j/\eta_1)\sin(j\Omega t + \Psi_j)}{(1-x)^2} \right\}$$

substrate at x=1

overall excitation amplitude

$\gamma>0$ magnitude of the electrostatic force, ≈ the square of the constant (DC) input voltage

Ω frequency of the periodic electrodynamic force

$\eta_j>0$ and Ψ_j : relative amplitudes and phases of the j-th harmonic of the electrodynamic force, i.e., of the oscillating (AC) voltage

MEMS: reference response chart (harmonic excitation)

- many bifurcation diagrams built

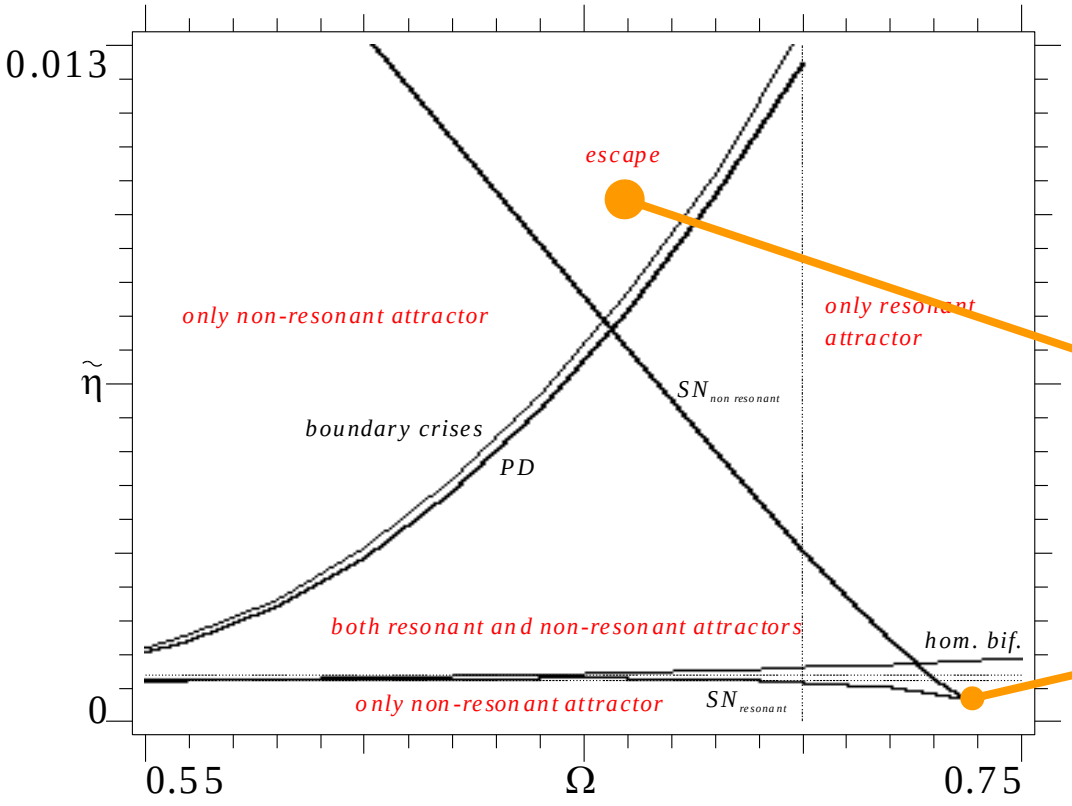

- same qualitative features of the Helmholtz oscillator
- V-shaped region of escape (dynamic pull-in), vertex at Ω=0.655
- degenerate cusp bifurcation at Ω=0.737 and η=0.000461

MEMS: basins erosion (harmonic excitation)

- classical basins of attraction (stationary regime)

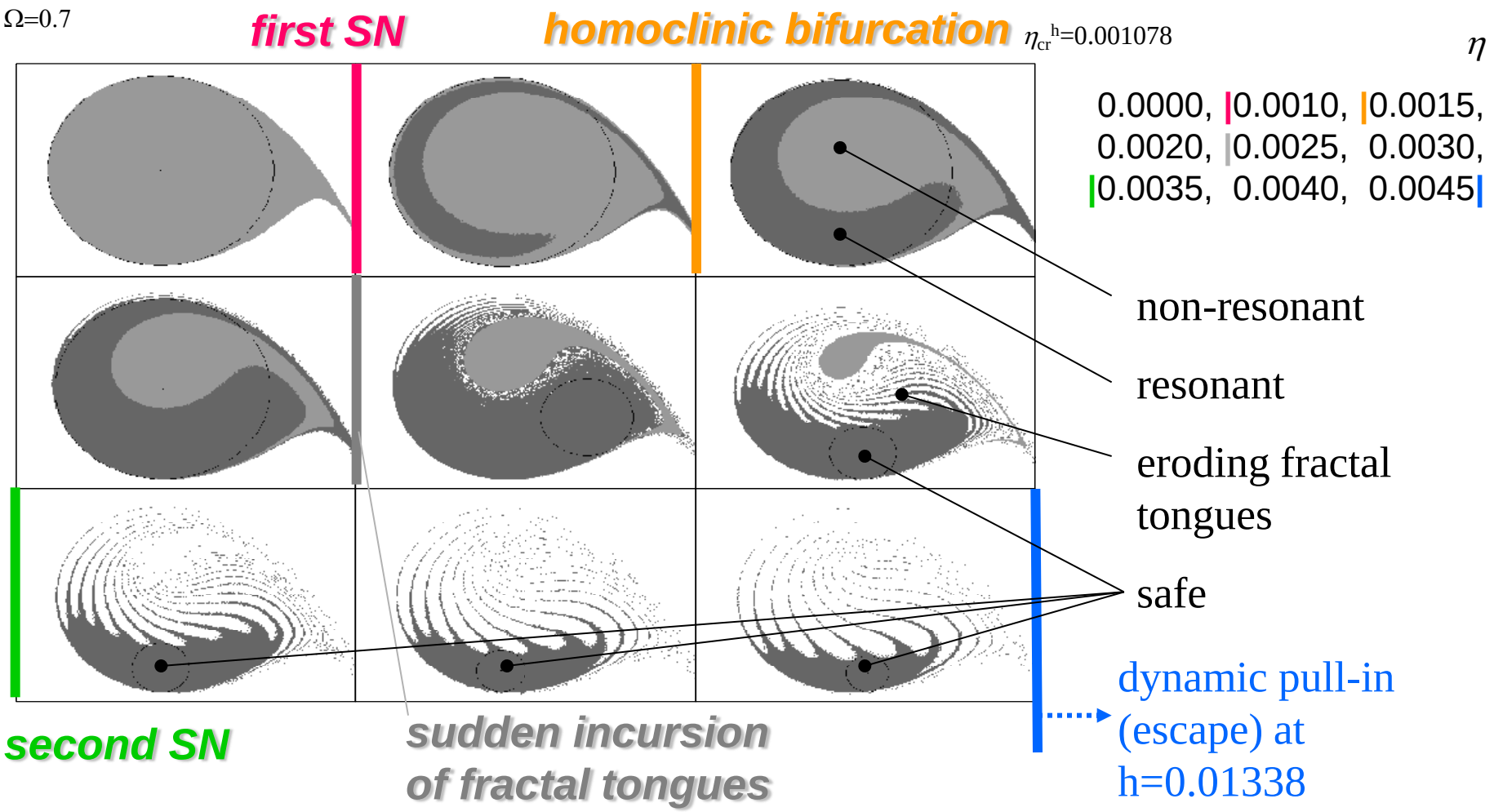

MEMS: erosion profiles (harmonic excitation)

- comparison of erosion profiles with Integrity Factor (I.F.) and Global Integrity Measure (G.I.M.)

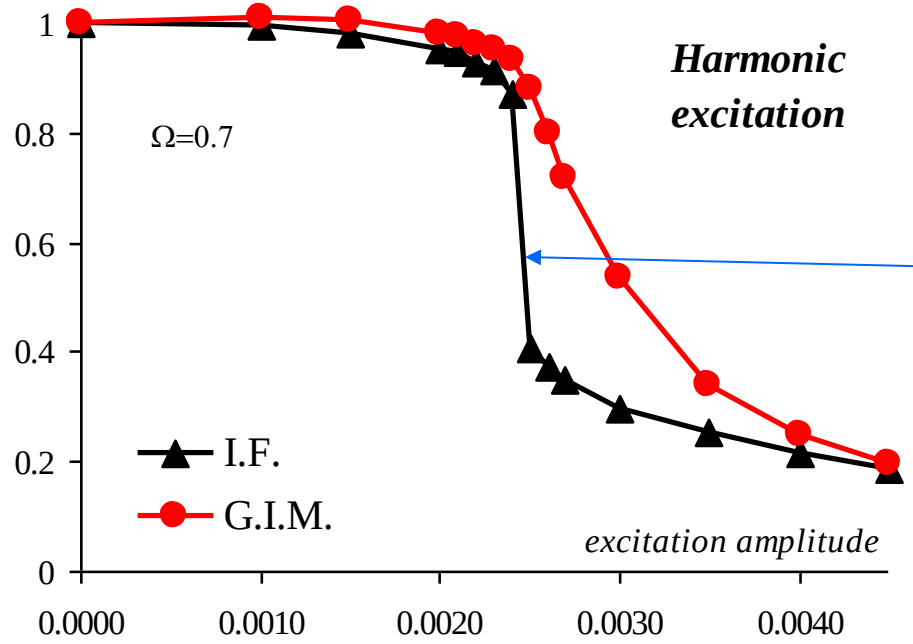

- I.F. better takes into account the instantaneous fractal tongues penetration
- I.F.<G.I.M. → I.F. more conservative → more reliable for practical applications

confirms rigid block results

MEMS: basin erosion (1) (fixed amplitude)

- effects of a single added superharmonic (N=2)

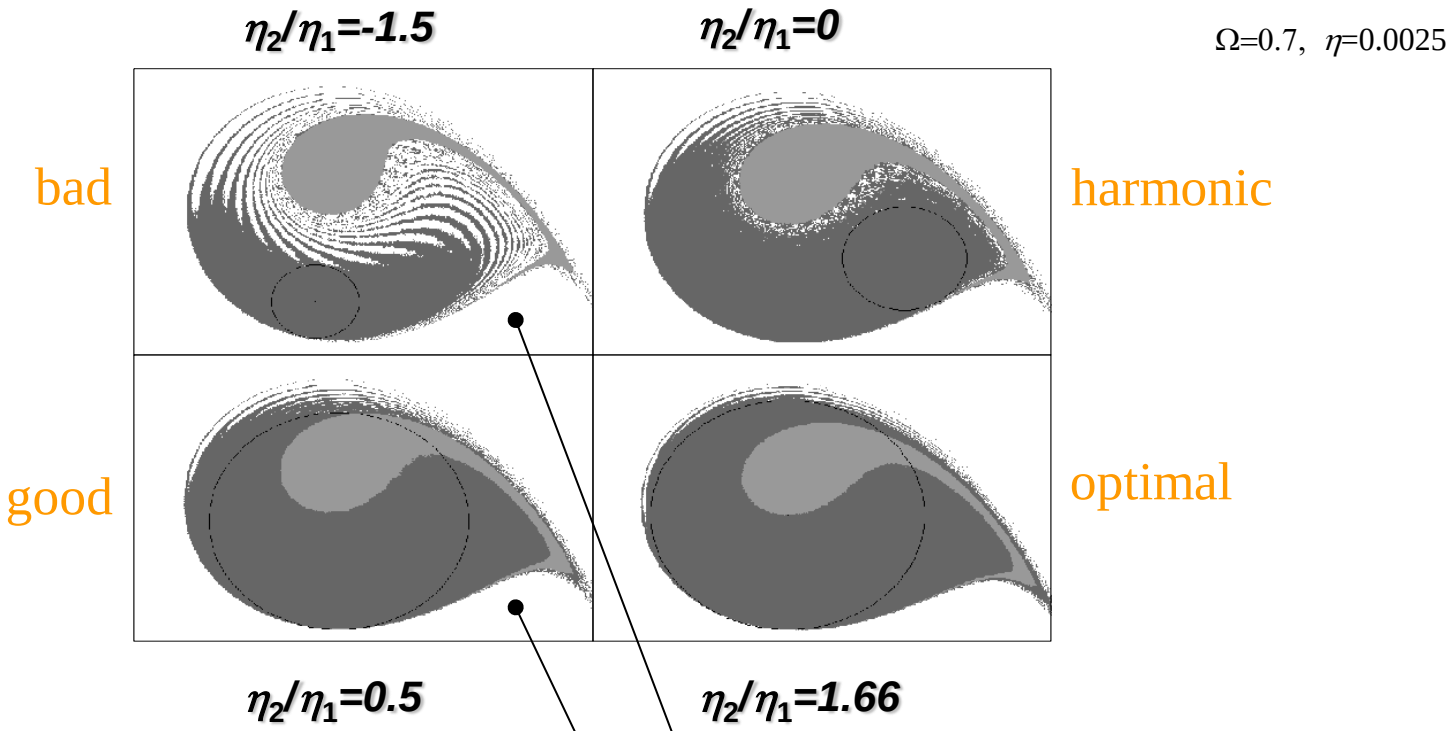

- the superharmonic may have dangerous effects if not properly designed
- good results also for non optimal superharmonic
- marginal increments around optimality

MEMS: basin erosion (2) (fixed amplitude)

Ω=0.7, η=0.0025

G = numerical (practical gains normalized to 1 (harmonic excitation) vs superharmonic relativeamplitude

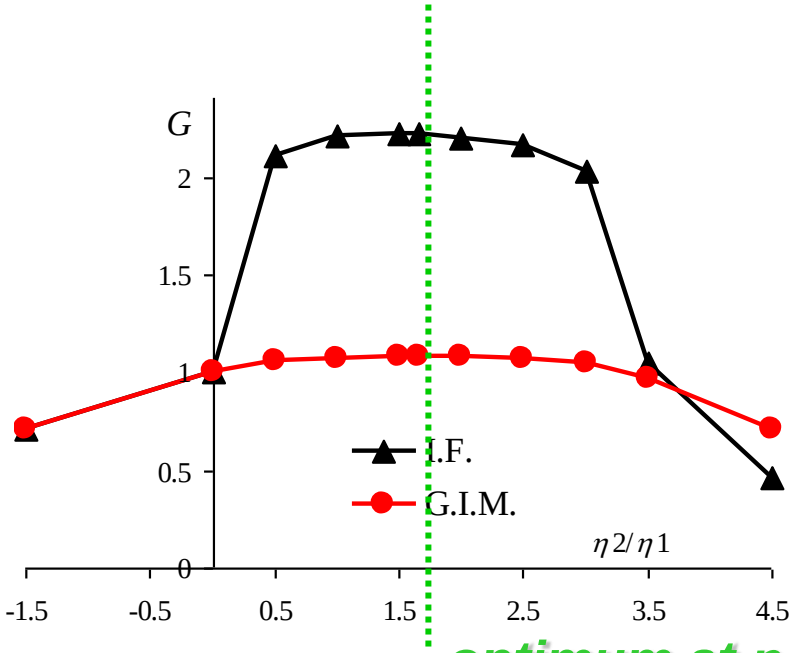

theoretical optimal superharmonic provides optimal practical results

G = theoretical gain as a function of superharmonic coefficient h2

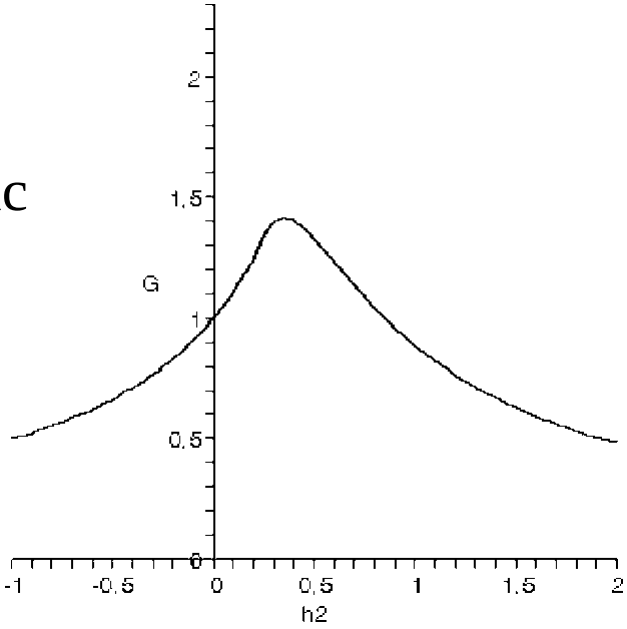

optimum at η_2/η_1=1.66

- almost optimal results on a broad band → practically appealing
- sharpness (I.F.) vs dullness (G.I.M.) due to different detection of instantaneous fractal penetration

MEMS: basin erosion (3) (varying amplitude)

- effects of superharmonics on erosion profiles

Ω=0.7

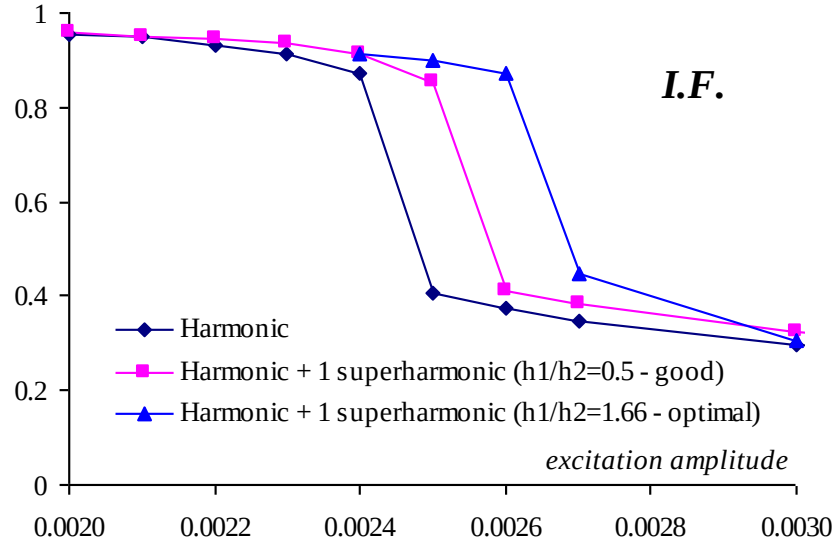

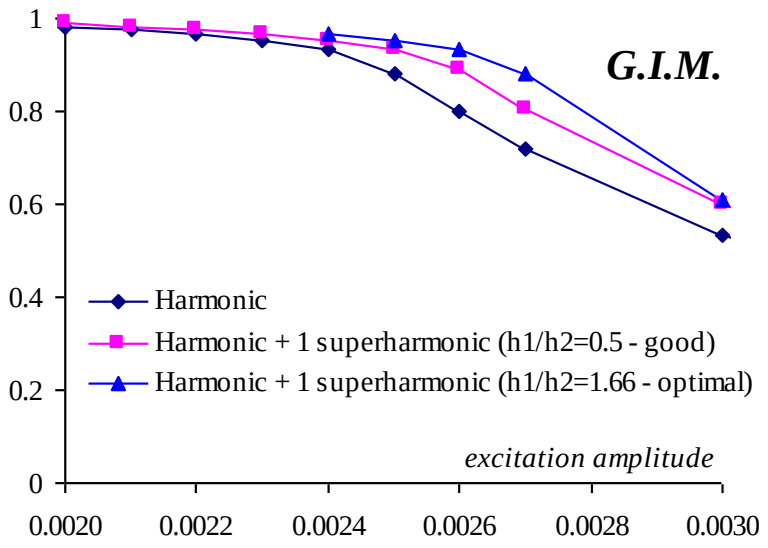

- shifting of erosion profiles
- same horizontal shift for both measures, different vertical shift (due to sharpness)
- profiles shapes maintained by superharmonics

Augusti's 2-d.o.f model (4D)

perfect system

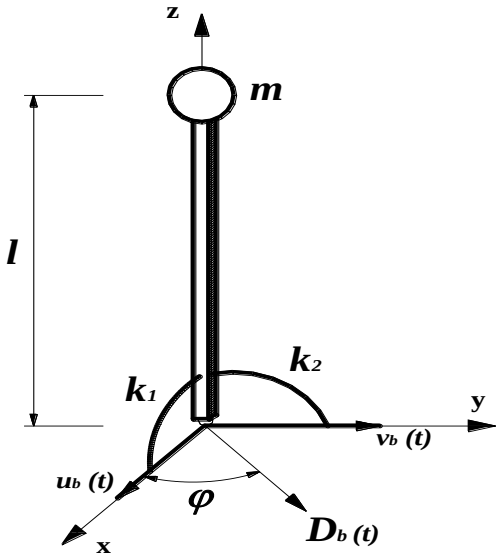

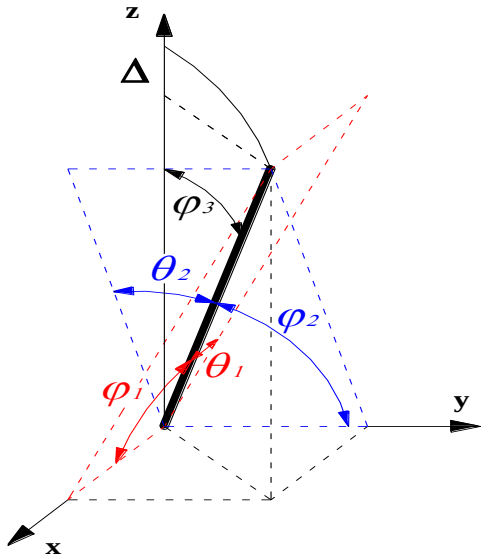

geometrically imperfect system

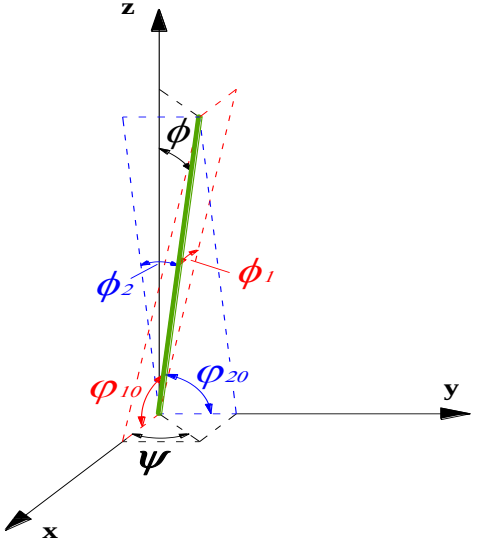

undeformed

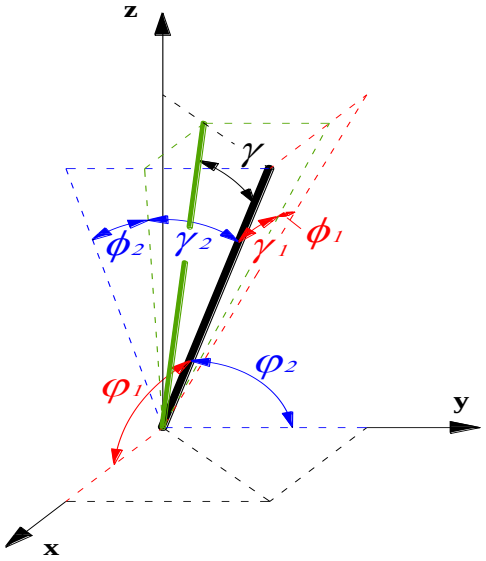

deformed

Augusti's 2-d.o.f. model (4D)

Perfect (static load $\lambda = 0.9$)

Equilibrium paths

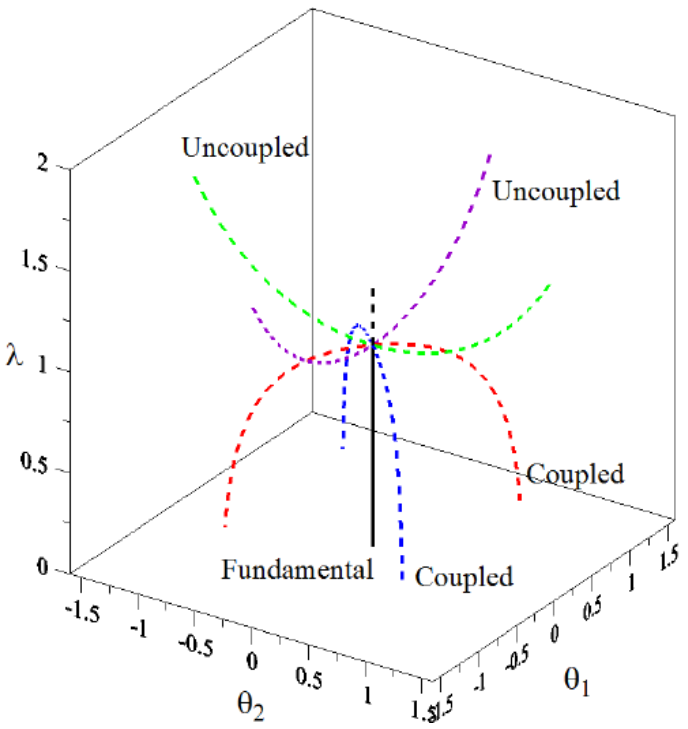

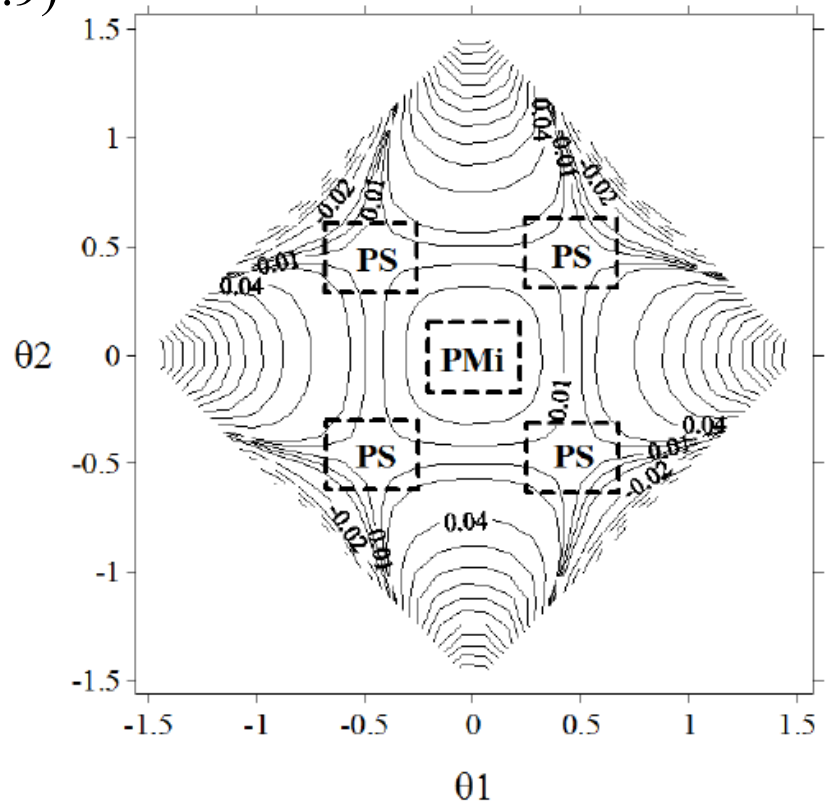

- four symmetric saddles ⟷ four **unstable postbuckling** descending branches
- minimum point ⟷ **stable prebuckling** solution

invariant manifolds of saddles separate i.c. leading to bounded solutions that surround the prebuckling configuration, and identify the **safe region**, from **unbounded escape** solutions

Augusti: Integrity 2D (on s.d.o.f. ROM)

Perfect case ($\Omega = 0.2465$, $\lambda = 0.9$ and $\xi = 0.01$)

***F*=0.60**

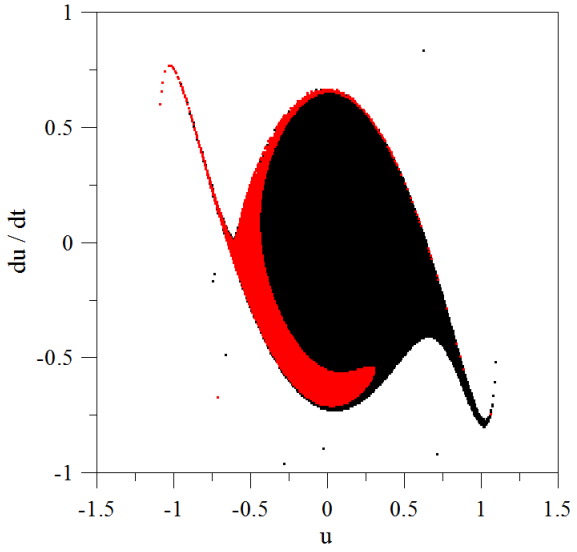

***F*=0.66**

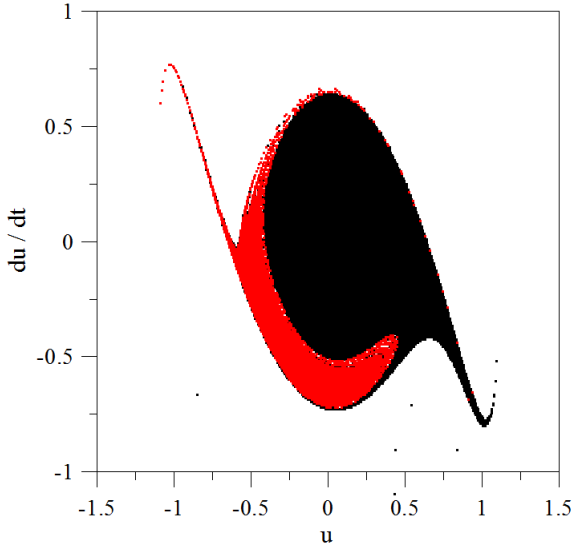

***F*=0.70**

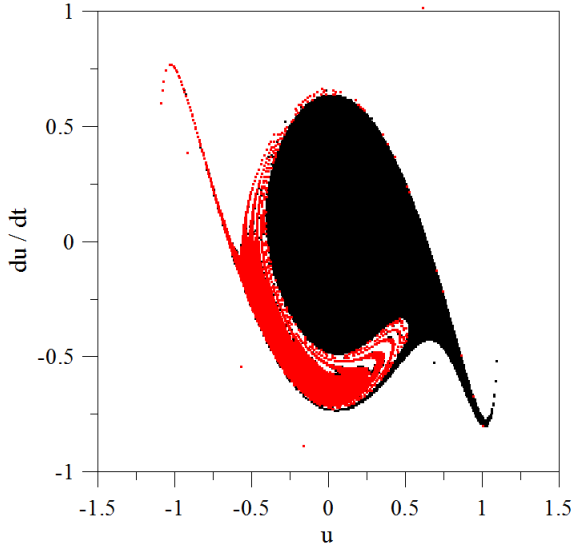

Erosion proceeds for increasing excitation amplitude *F*

Augusti: Integrity 2D (on s.d.o.f. ROM)

($\lambda = 0.9$ and $\xi = 0.01$)

❖ **Map of the local bifurcations in the fundamental resonance region prior to escape:**

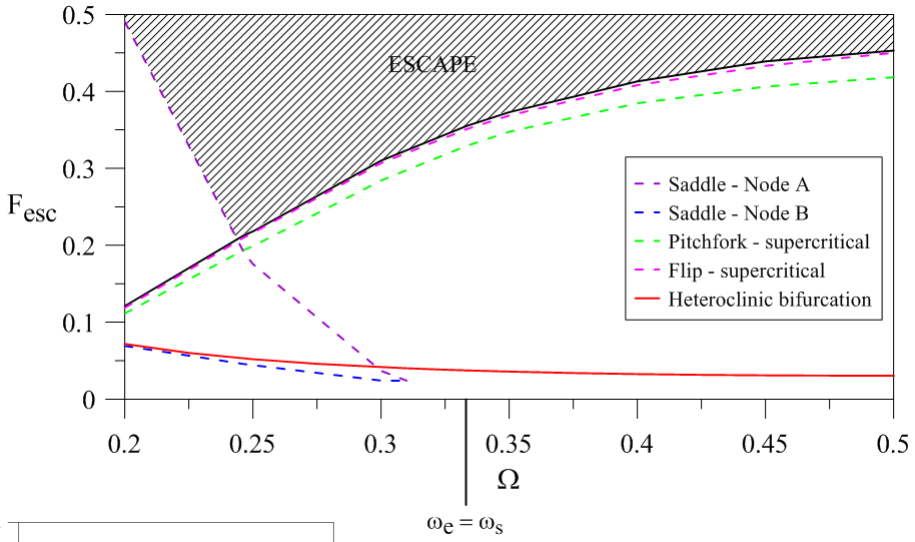

Perfect case

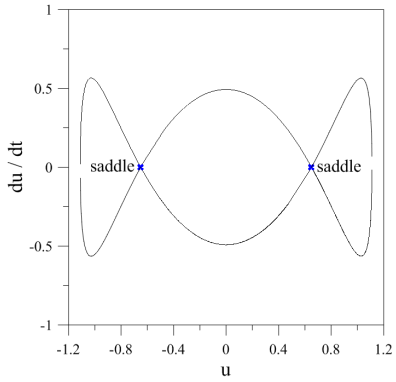

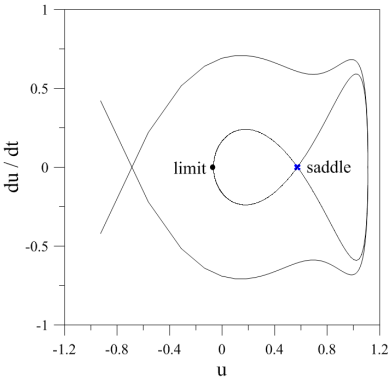

Imperfect case ($u_{10} = 1°$)

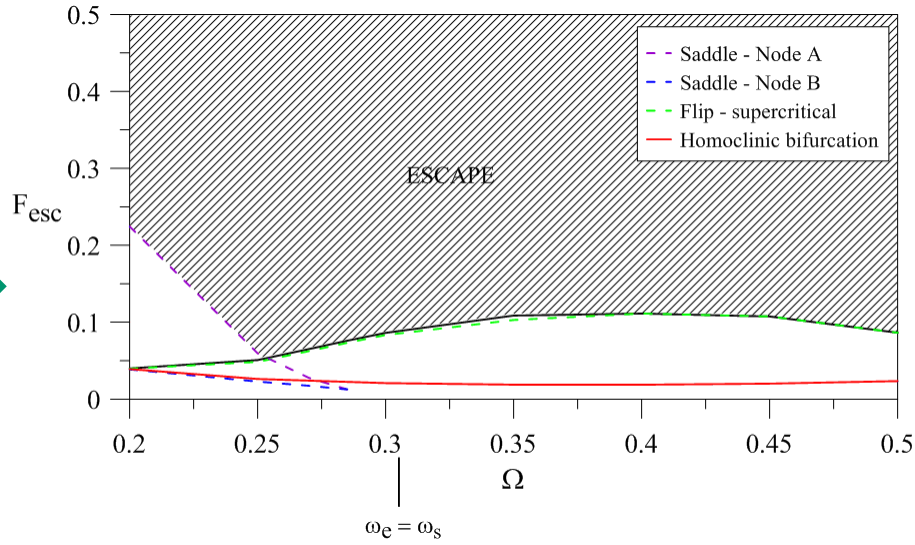

Augusti: Integrity 2D (on s.d.o.f. ROM)

$(\lambda = 0.9 \text{ and } \xi = 0.01)$

❖ **Integrity profiles:**

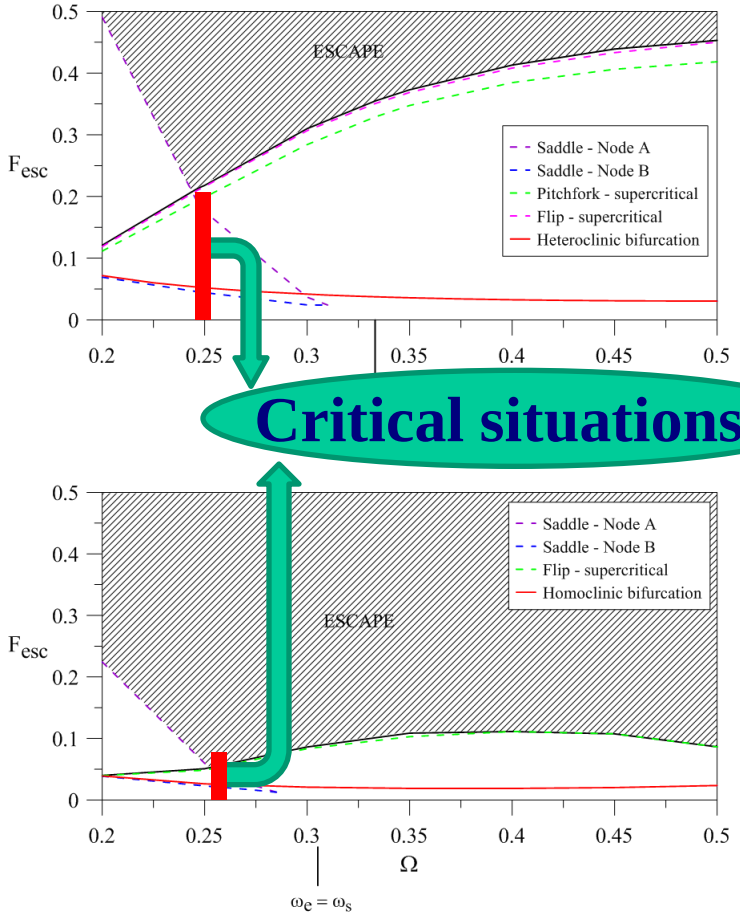

Critical situations

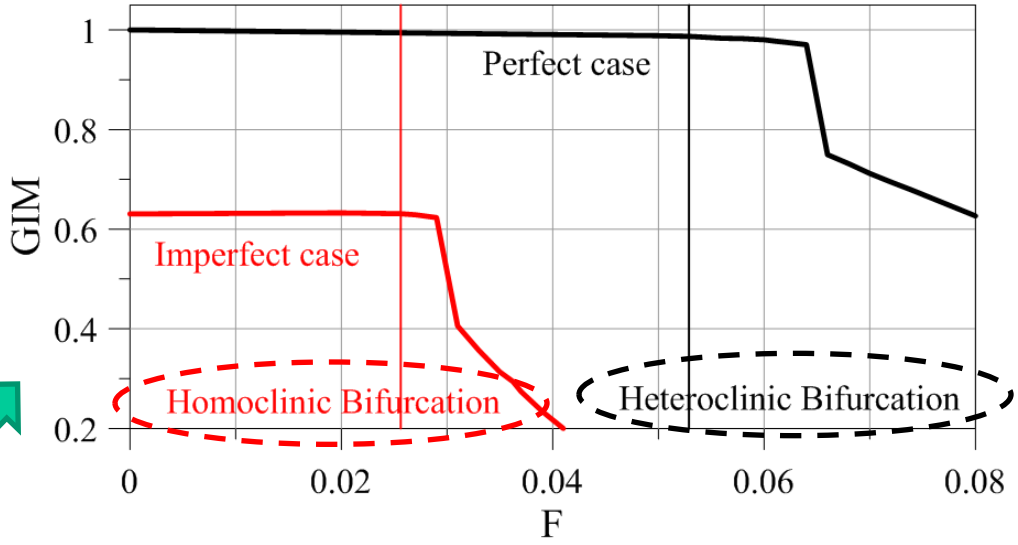

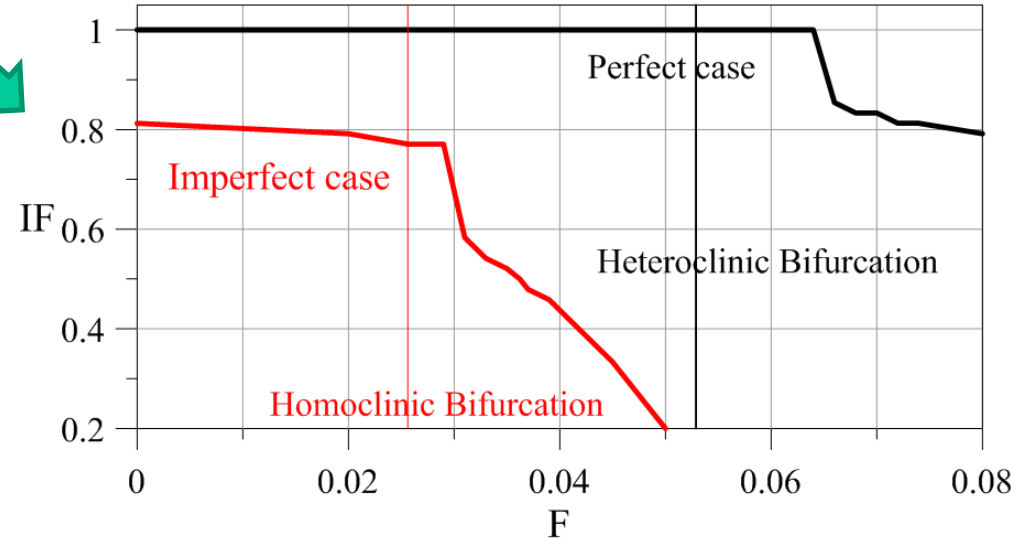

Augusti's model: control strategy

$(\lambda = 0.9)$

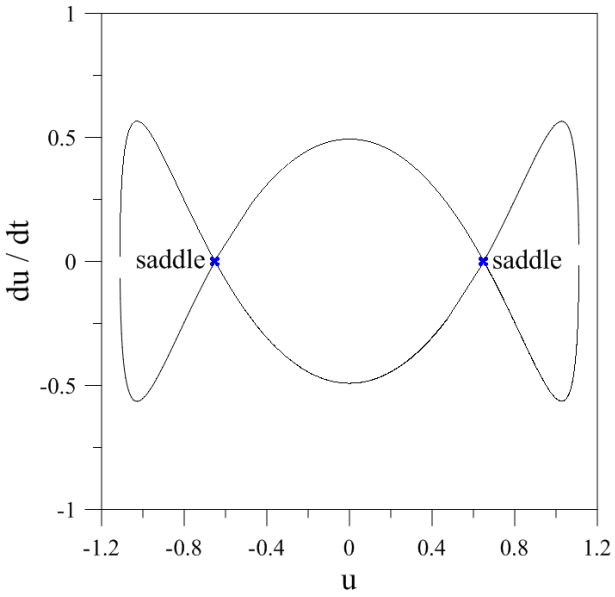

Perfect case (heteroclinic orbit) → global control (addition of a super-harmonic of order 3 to the harmonic excitation of the system)

Imperfect case (homoclinic orbit) → one-side control (addition of a super-harmonic of order 2 to the harmonic excitation of the system)

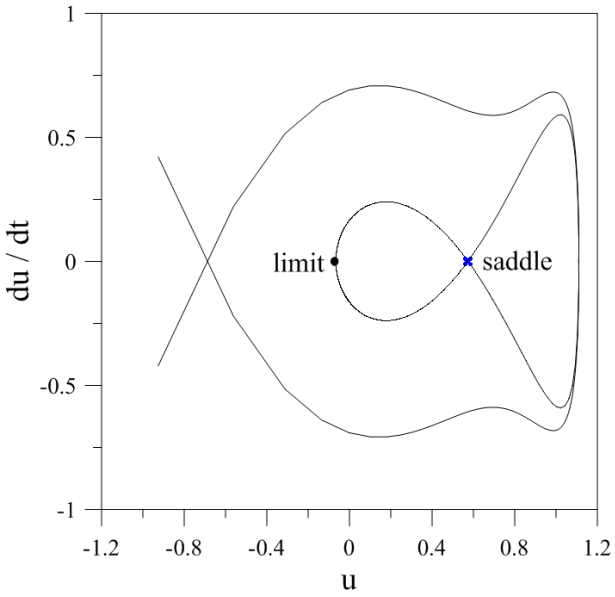

Augusti's model: control excitations

New excitation

$$F\left(\cos\left(\frac{u\sqrt{2}}{2}\right)\sin(\tau)+\right.$$

$$\left.\frac{F_3}{F}\cos\left(\frac{u\sqrt{2}}{2}\right)\sin(3\tau+\nu_3)\right)$$

Perfect case (heteroclinic orbit) → global control (addition of one super-harmonic of order 3 to the harmonic excitation of the system)

Imperfect case (homoclinic orbit) → one-side control (addition of one super-harmonic of order 2 to the harmonic excitation of the system)

New excitation

$$F\left(\cos\left(\frac{u\sqrt{2}}{2}\right)\sin(\tau)+\right.$$

$$\left.\frac{F_2}{F}\cos\left(\frac{u\sqrt{2}}{2}\right)\sin(2\tau+\nu_2)\right)$$

Augusti's model: local effectiveness of control

$(\lambda = 0.9 \text{ and } \xi = 0.01)$

Uncontrolled model →

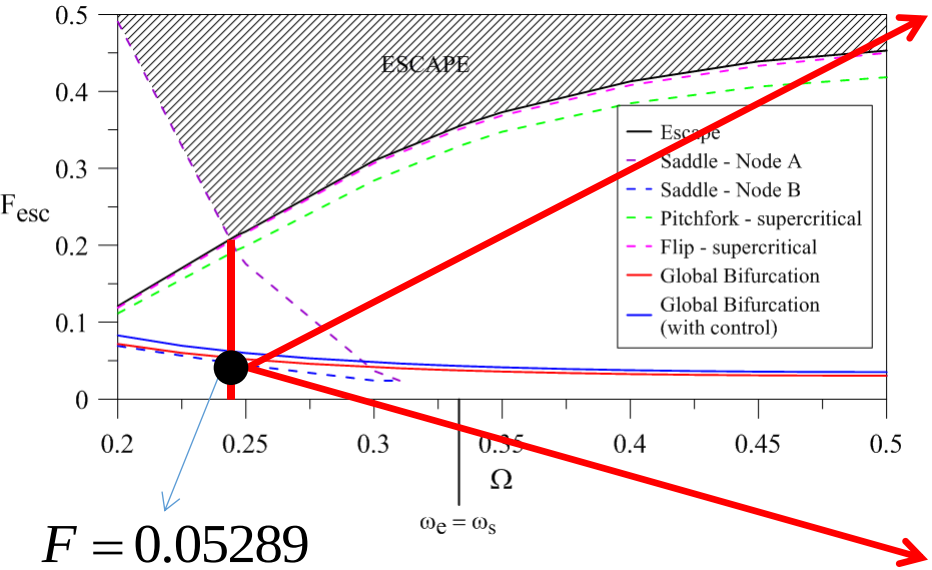

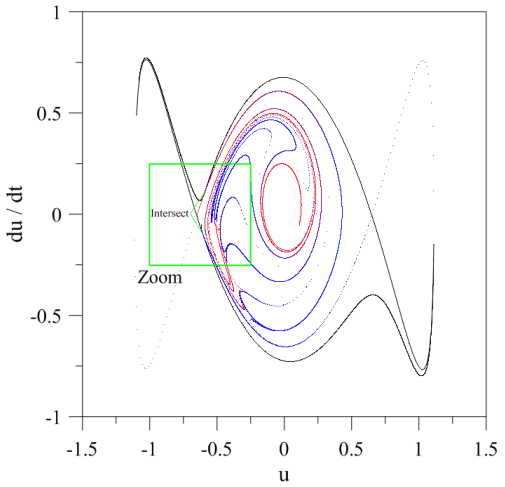

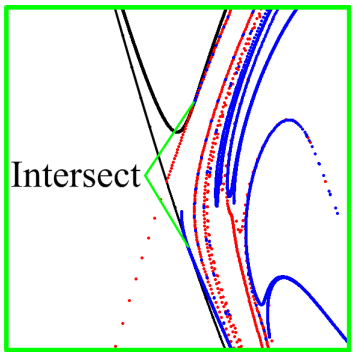

Controlled model →

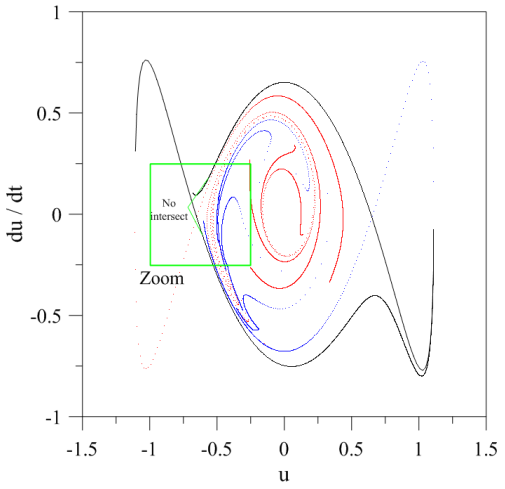

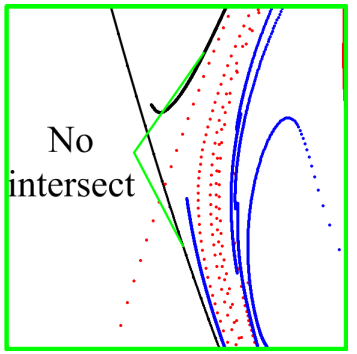

❖ Theoretical **gain of 15.47%**

Augusti's model: comparison of integrity profiles

Perfect case ($\Omega = 0.2465$, $\lambda = 0.9$ and $\xi = 0.01$)

Both GIM and IF show the effectiveness of control

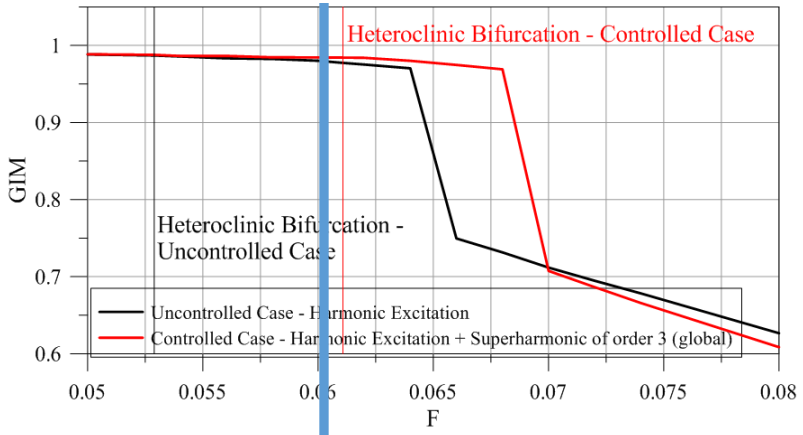

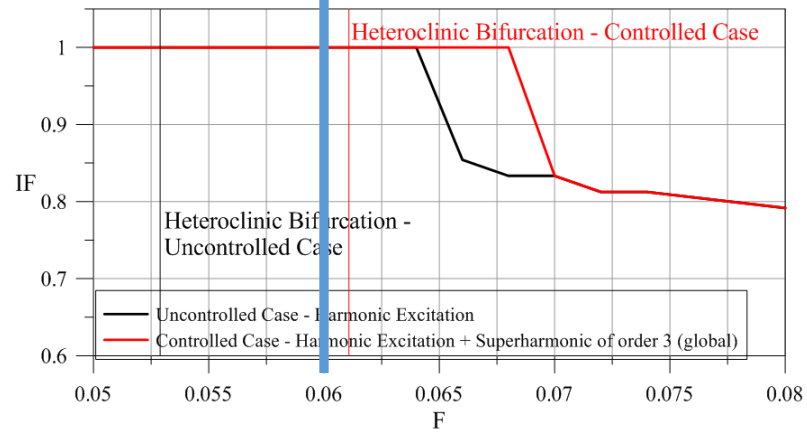

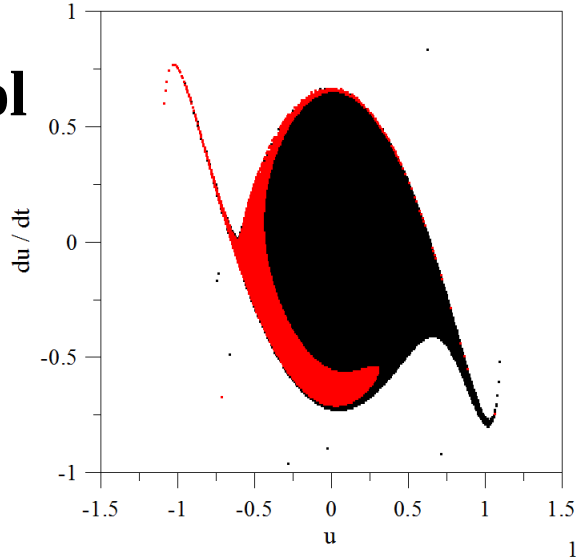

Uncontrolled model

Controlled model

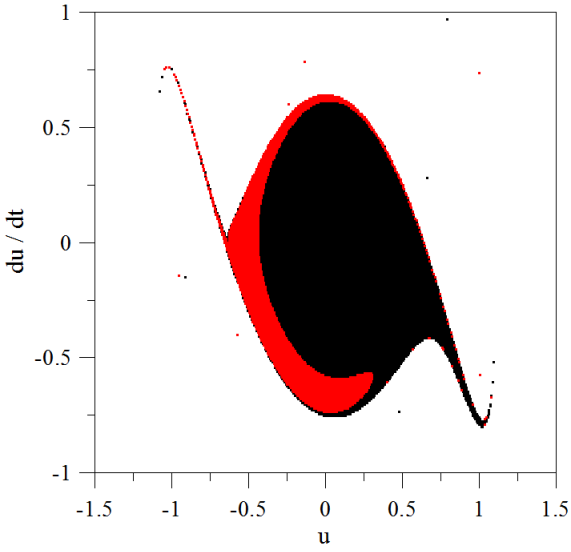

Augusti's model: comparison of integrity profiles

Perfect case ($\Omega = 0.2465$, $\lambda = 0.9$ and $\xi = 0.01$)

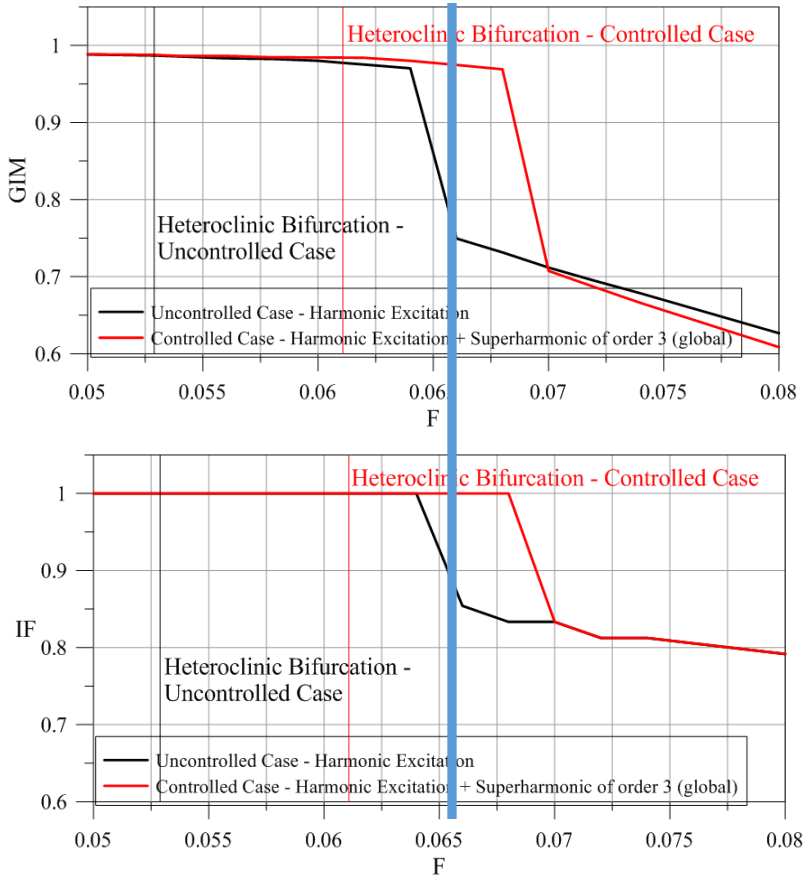

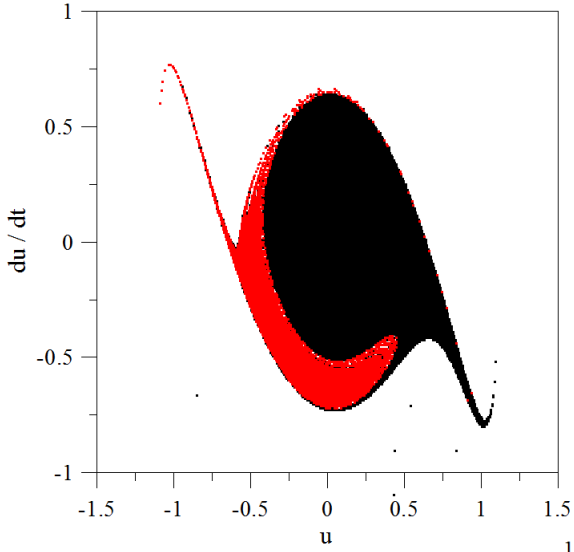

Uncontrolled model

Controlled model

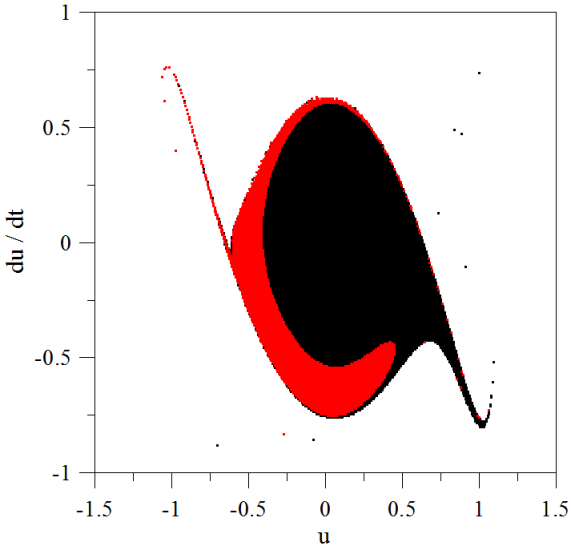

Augusti's model: comparison of integrity profiles

Perfect case ($\Omega = 0.2465$, $\lambda = 0.9$ and $\xi = 0.01$)

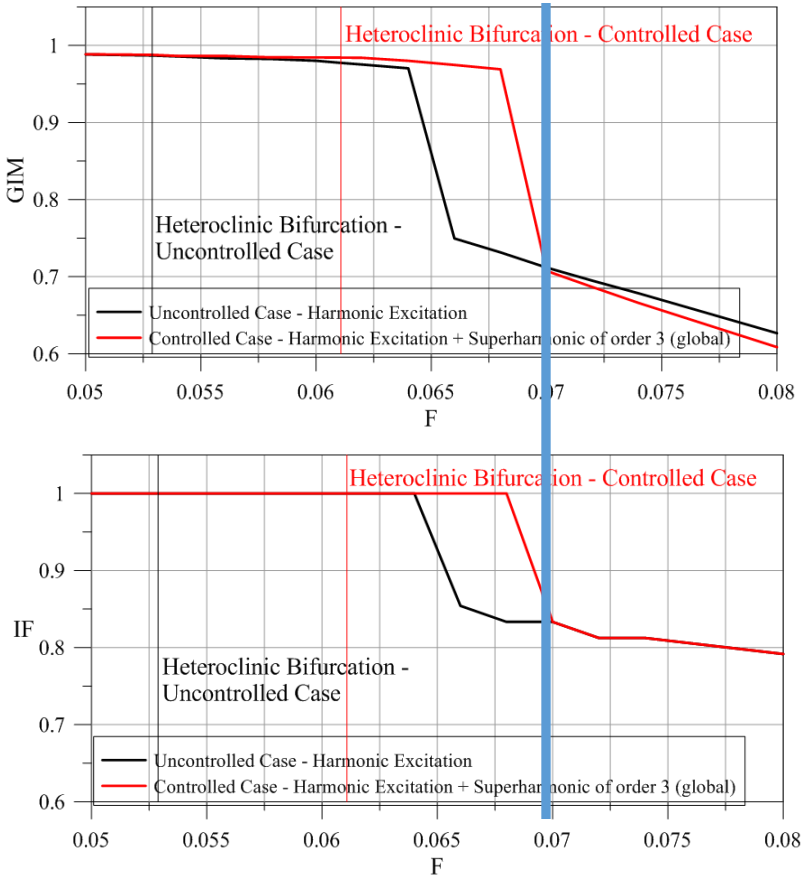

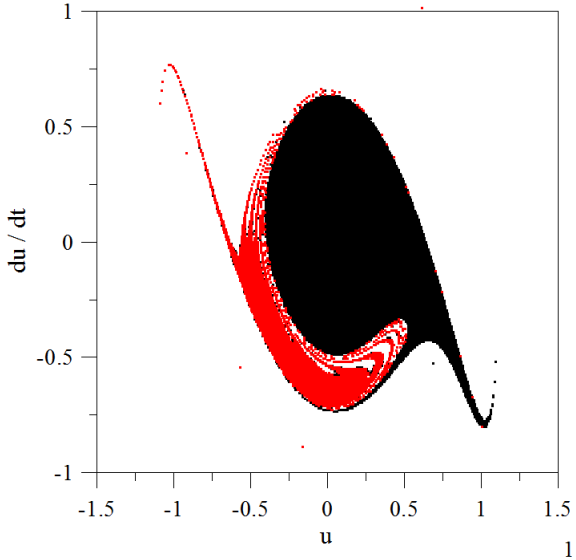

Uncontrolled model

Controlled model

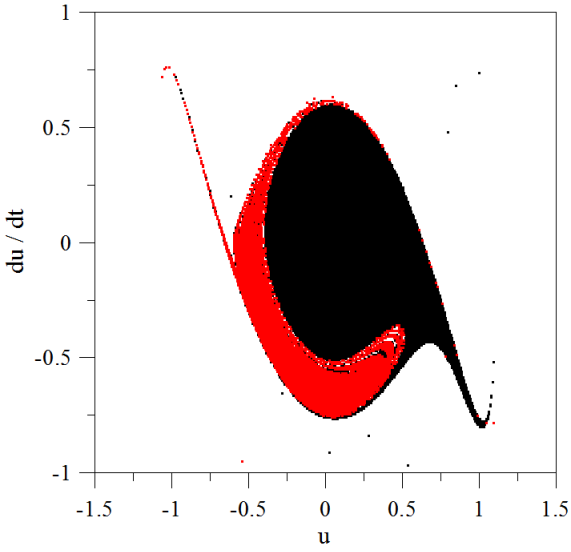

Augusti's model: local effectiveness of control

Imperfect case ($\lambda = 0.9$, $u_{10} = 1°$ and $\xi = 0.01$)

Uncontrolled model →

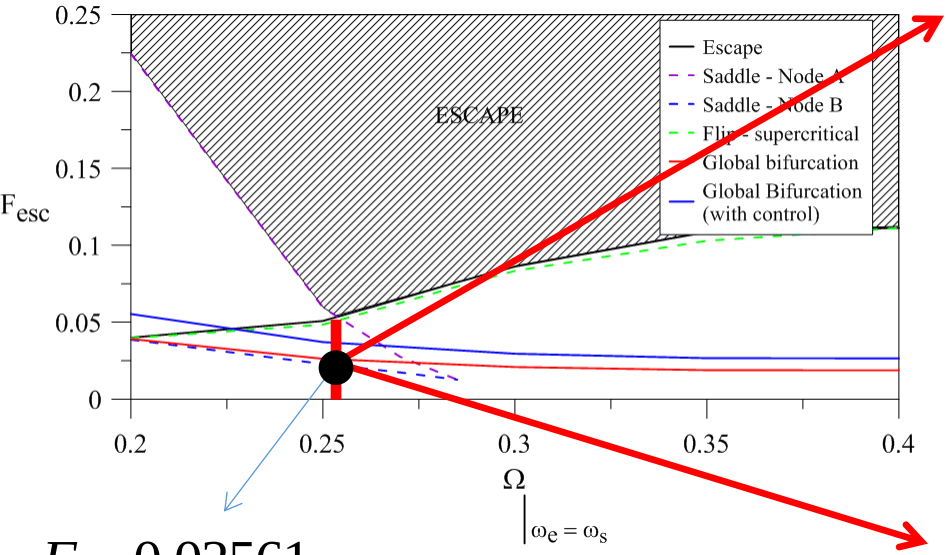

$F = 0.02561$

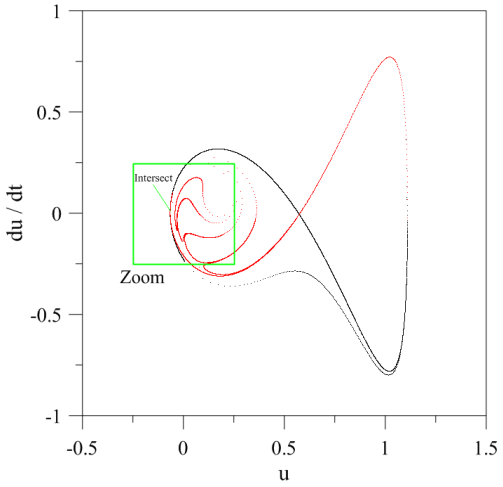

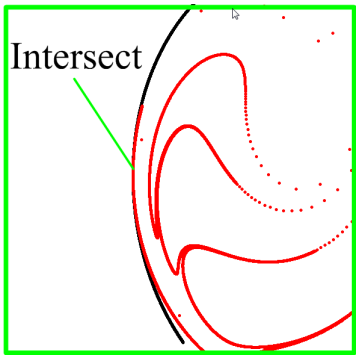

Controlled model →

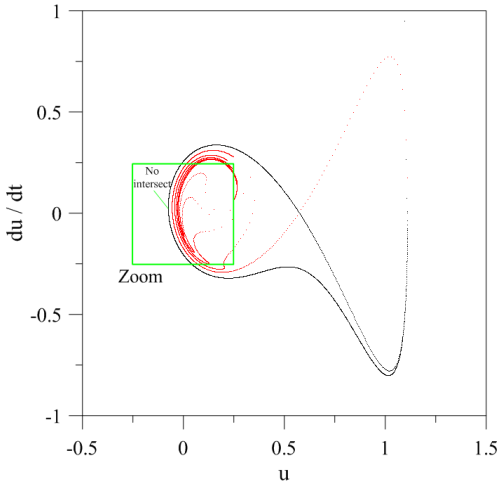

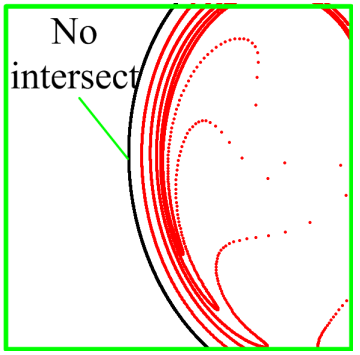

❖ Theoretical **gain of 41.42%**

Augusti's model: comparison of integrity profiles

Imperfect case ($\Omega = 0.254$, $\lambda = 0.9$, $u_{10} = 1°$ and $\xi = 0.01$)

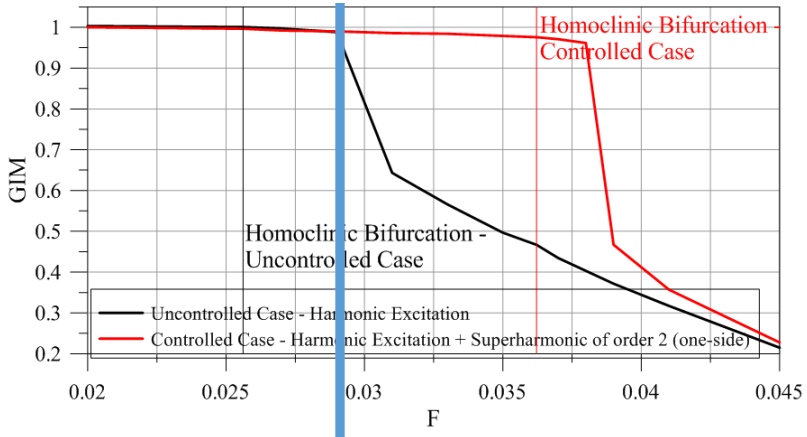

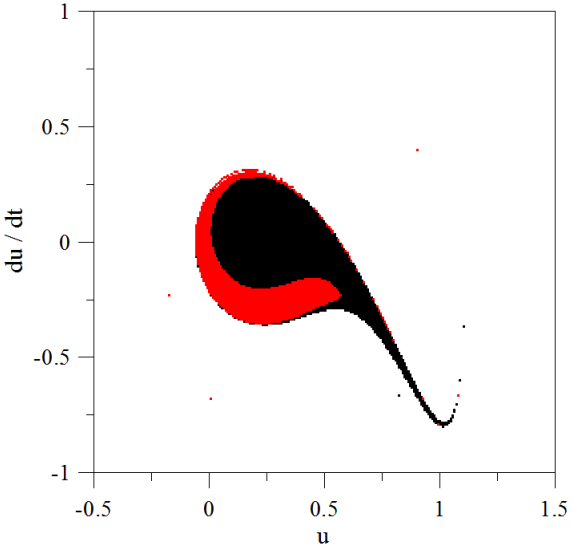

Uncontrolled model

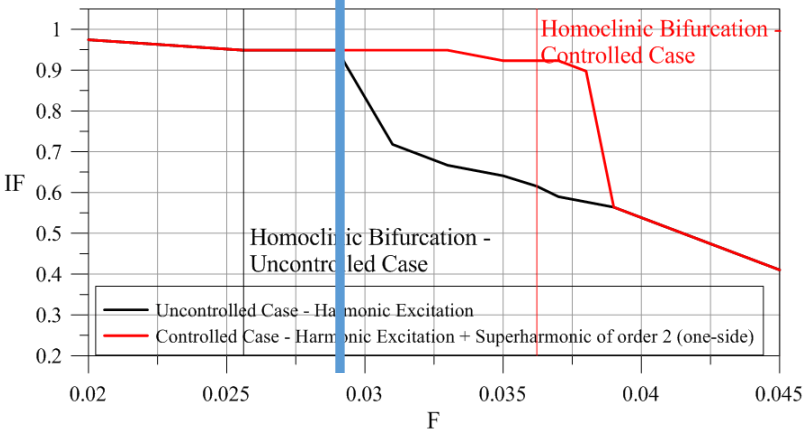

Controlled model

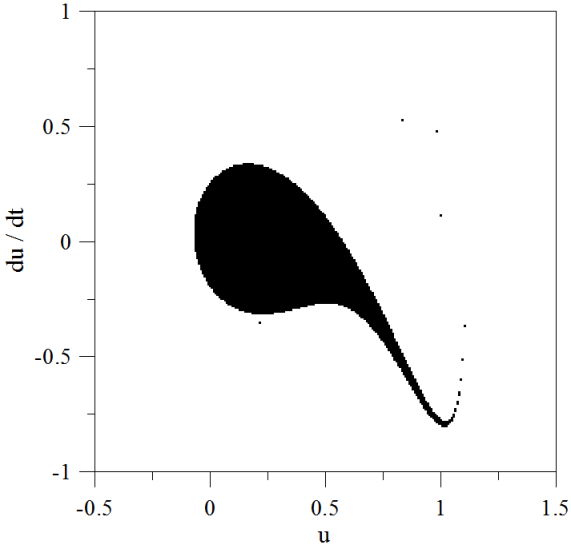

Augusti's model: comparison of integrity profiles

Imperfect case ($\Omega = 0.254$, $\lambda = 0.9$, $u_{10} = 1°$ and $\xi = 0.01$)

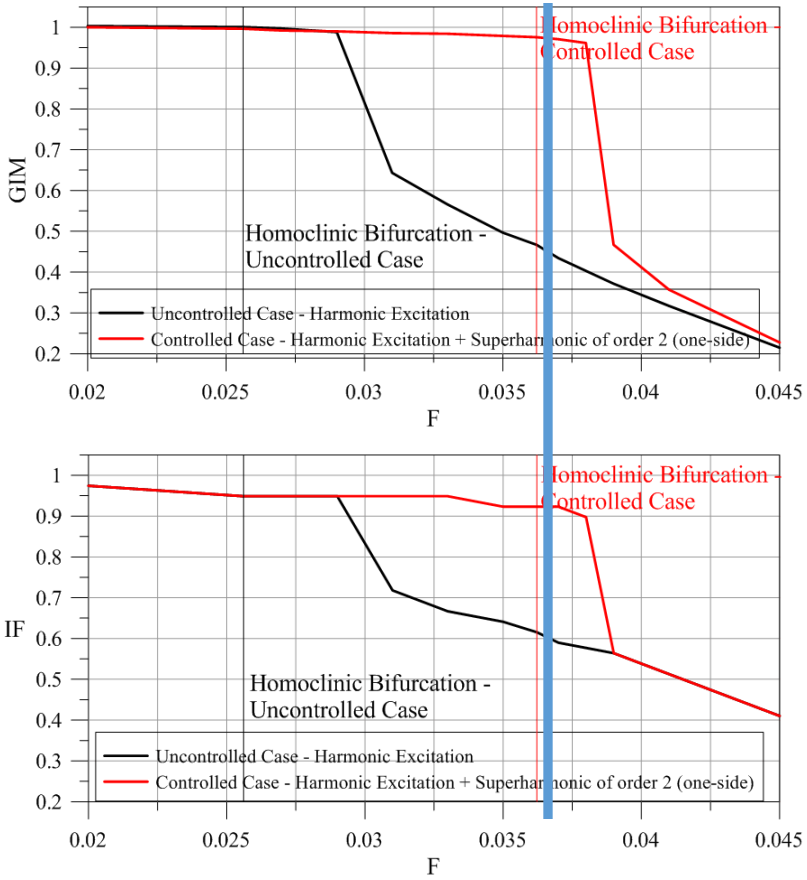

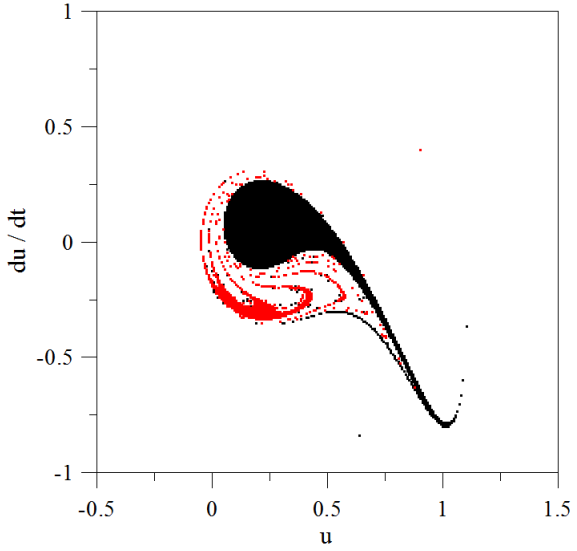

Uncontrolled model

Controlled model

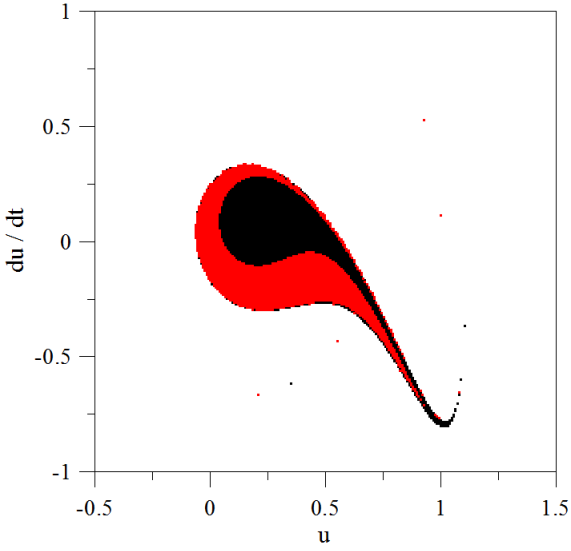

Augusti's model: comparison of integrity profiles

Imperfect case ($\Omega = 0.254$, $\lambda = 0.9$, $u_{10} = 1°$ and $\xi = 0.01$)

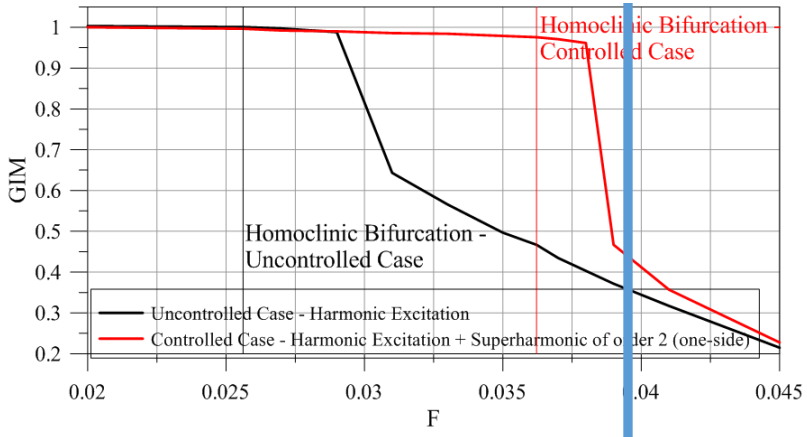

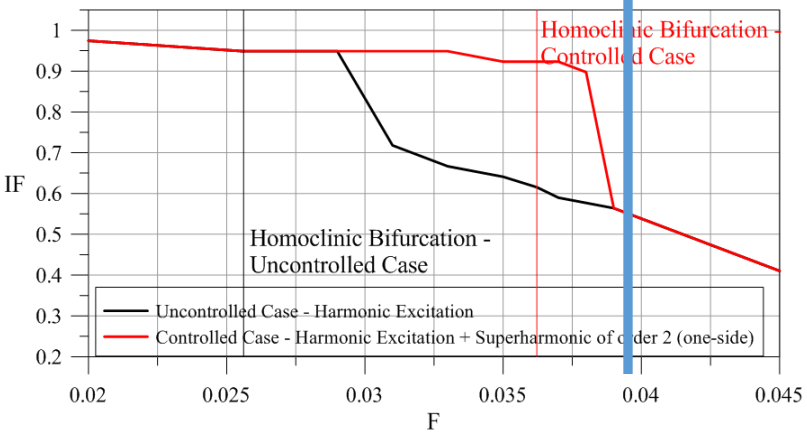

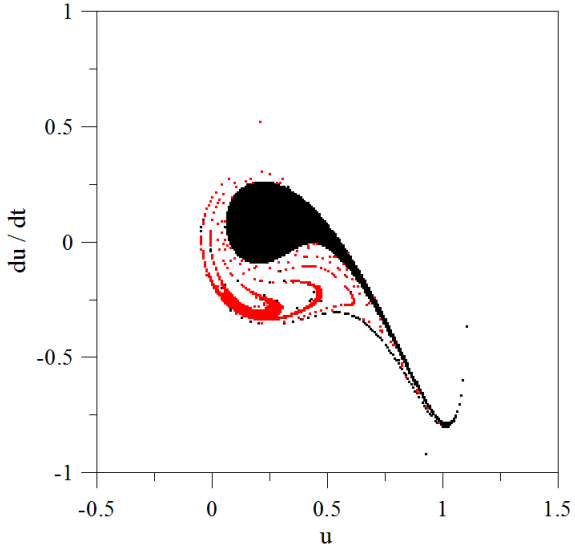

Uncontrolled model

Controlled model

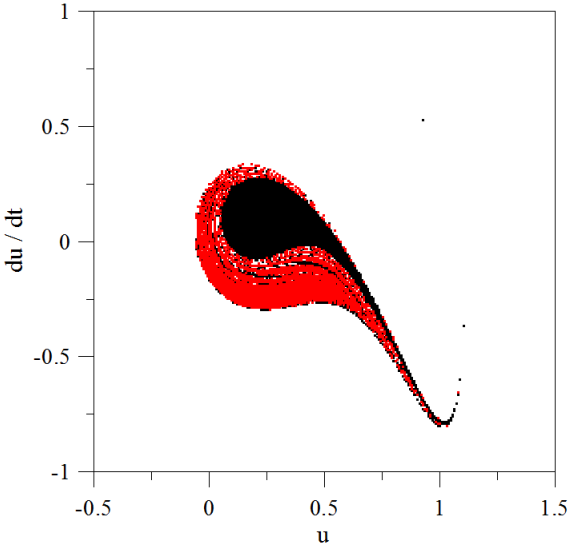

Augusti's model

Comparison of the perfect and imperfect systems:

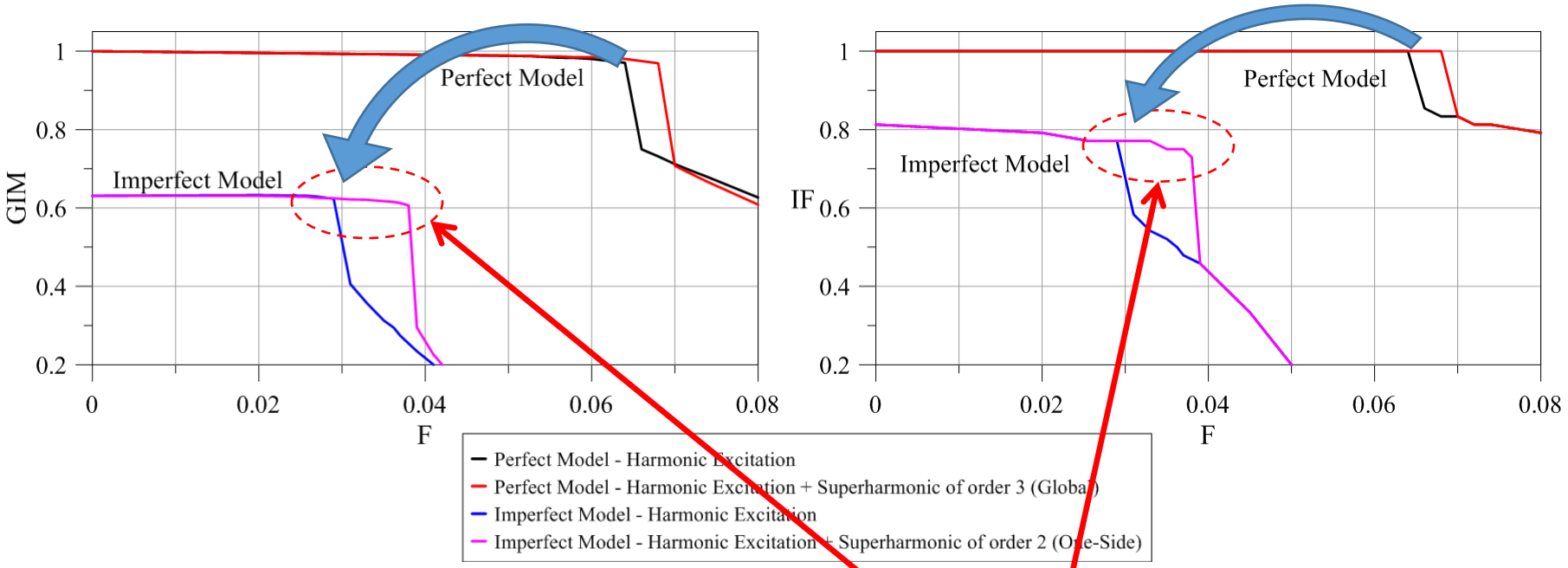

- Imperfection strongly reduces the system load carrying capacity
- Control is more effective where most needed (imperfect model)

Guyed tower 2-dof model (4D)

- The **simplified model of a guyed tower** is stabilized by three linear springs, k_1, k_2 and k_3, initially inclined at 45° and located symmetrically by 120°
- The model is under a harmonic base excitation $D_b(t)$ acting at an angle φ with respect to the x axis

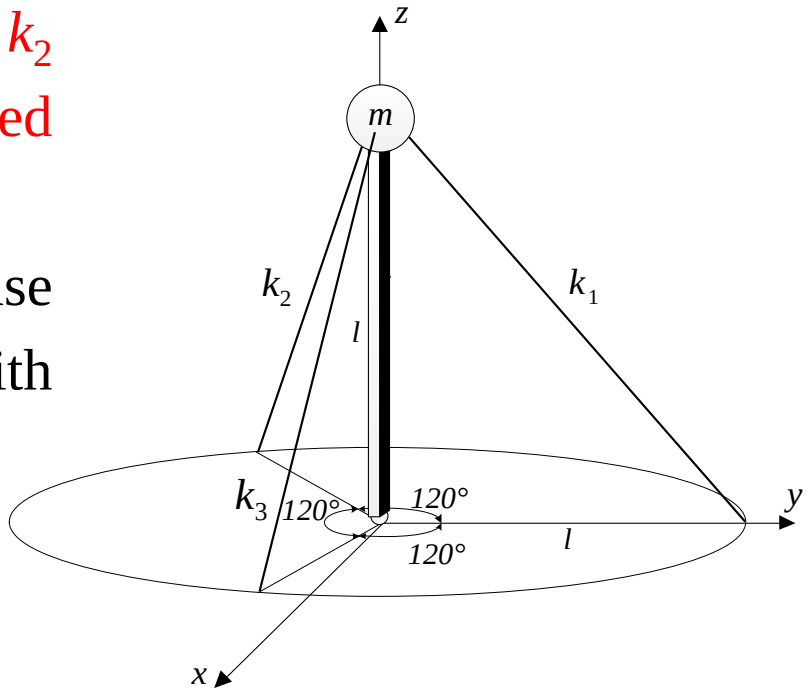

Guyed tower: Integrity 2D (on reduced order model)

($\lambda = 0.7$ and $\xi = 0.01$)

❖ **Map of the local bifurcations in the fundamental resonance region prior to escape:**

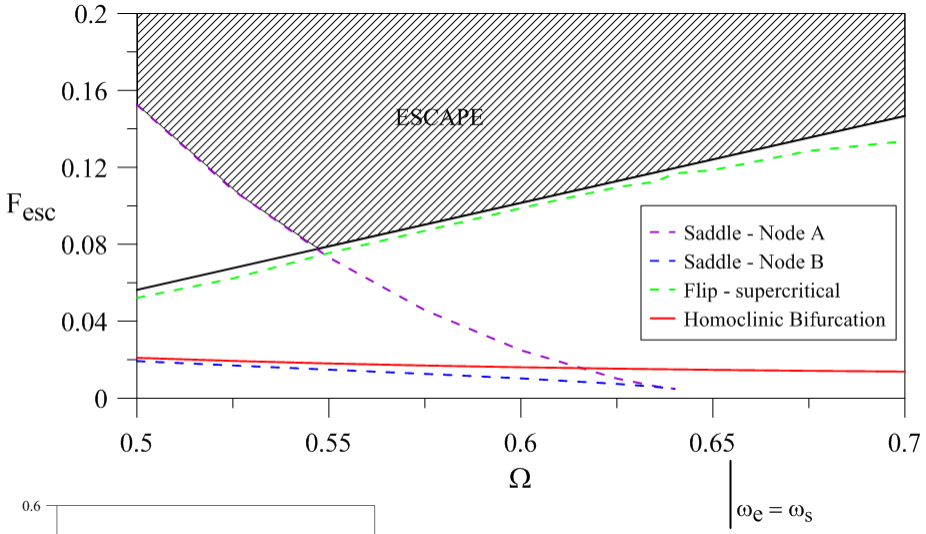

Perfect case

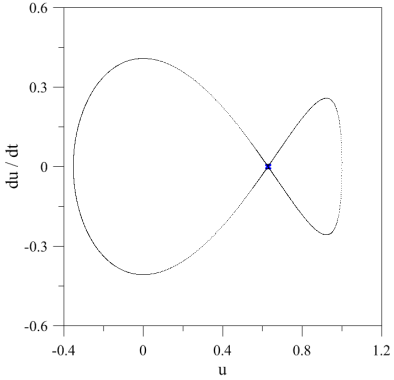

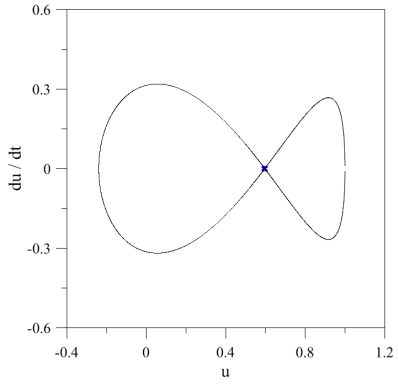

Imperfect case ($u_{10} = 1°$)

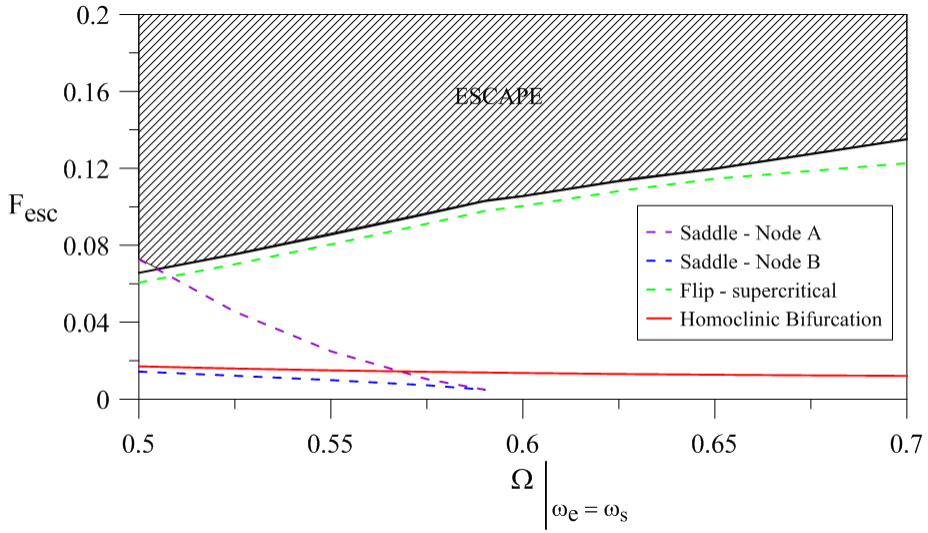

Guyed tower: Integrity 2D (on reduced order model)

($\lambda = 0.7$ and $\xi = 0.01$)

❖ **Integrity profiles:**

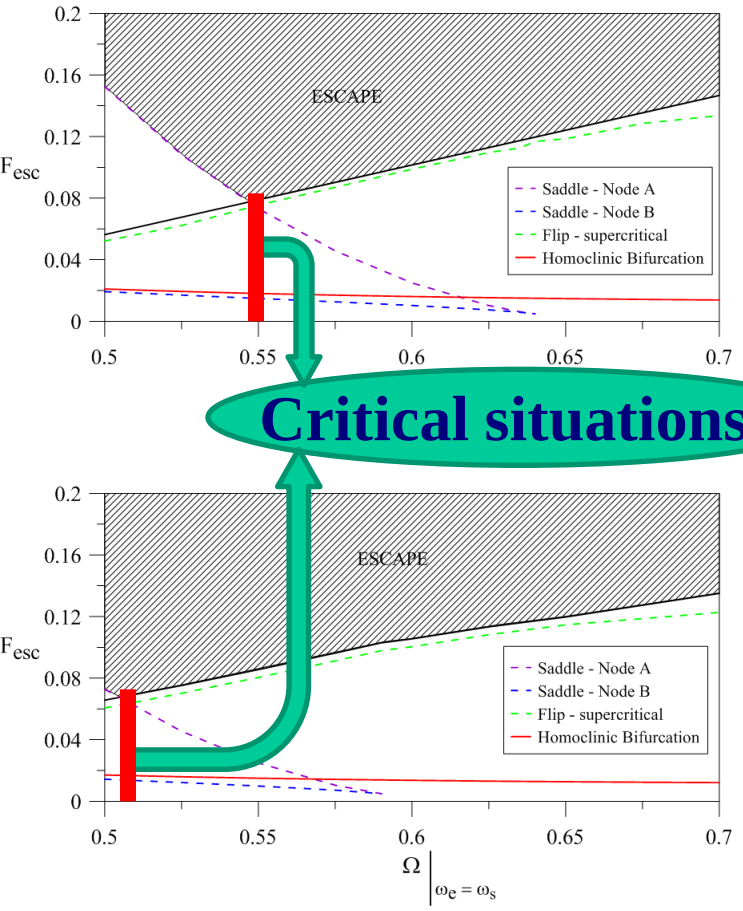

Critical situations

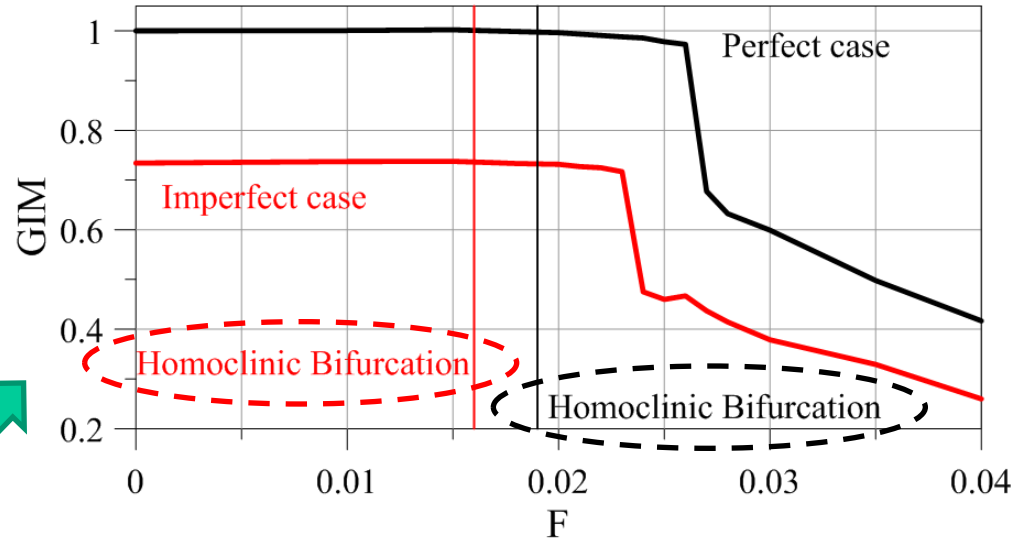

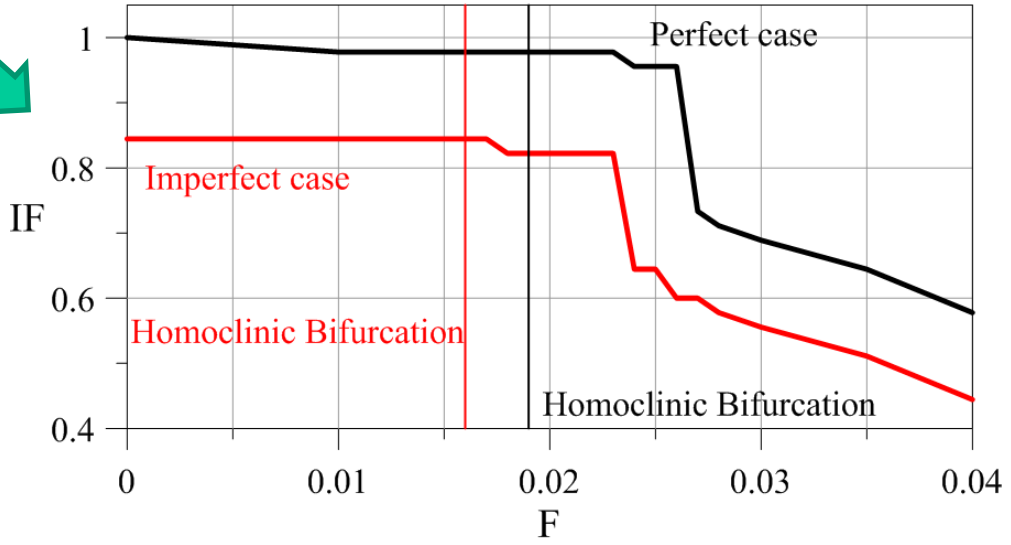

Guyed tower: one-side control

$(\lambda = 0.7)$

Control strategy:

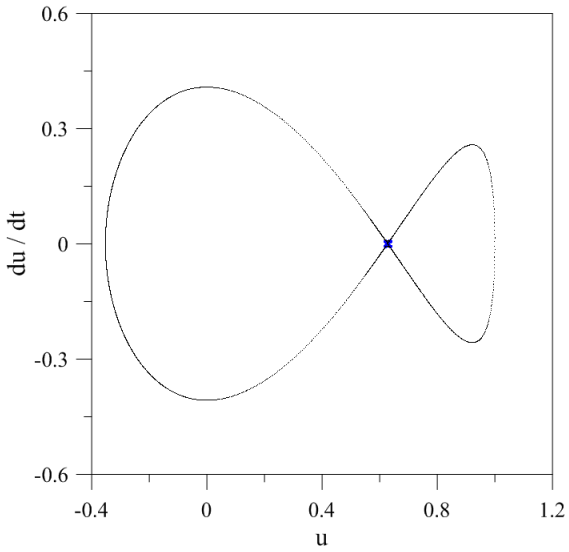

Perfect case

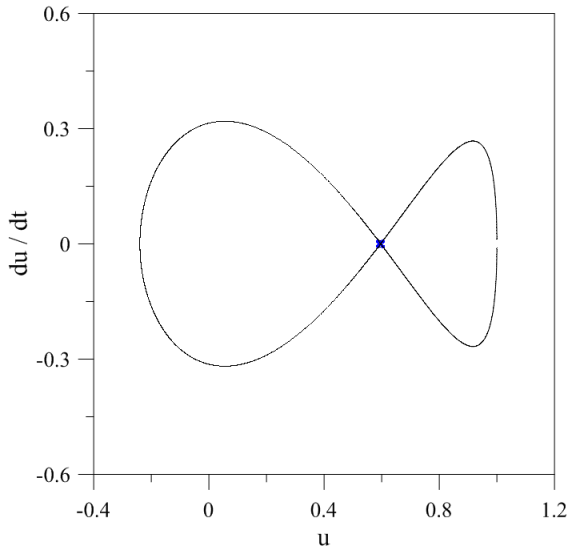

Imperfect case (u_{10} = 1°)

Homoclinic orbits → one-side control (addition of one super-harmonic of order 2)

New excitation

$$F\left(\sin(\tau)+\frac{F_2}{F}\sin(2\tau+\nu_2)\right)$$

Guyed tower: comparison of integrity profiles

Perfect case ($\Omega = 0.547$, $\lambda = 0.7$ and $\xi = 0.01$)

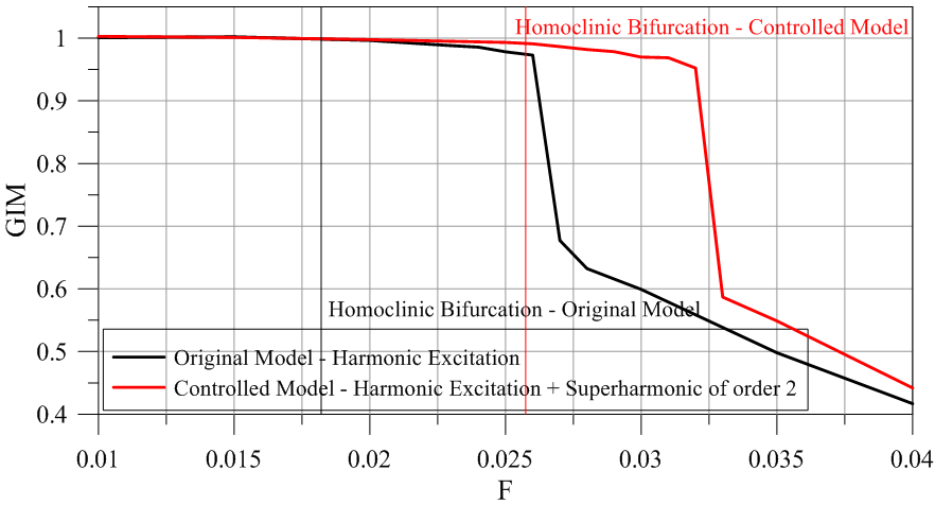

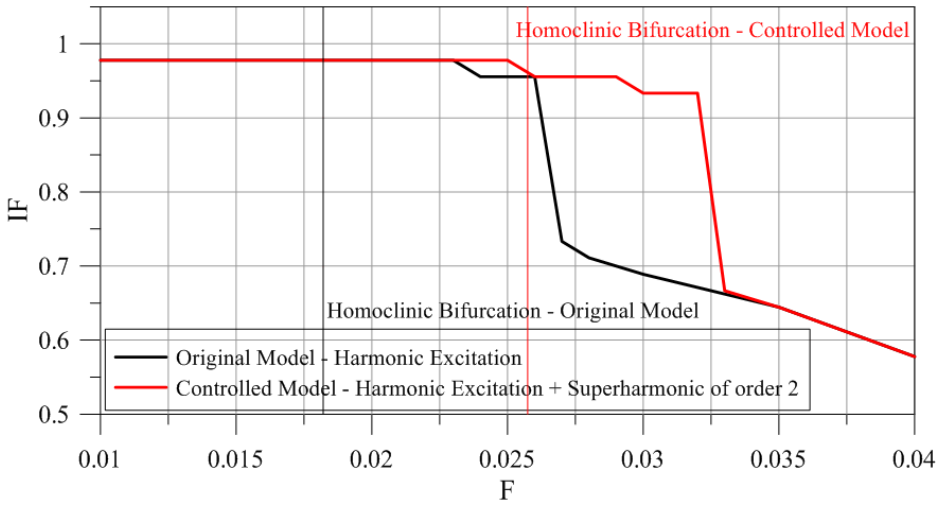

❖ Both GIM and IF show the increment of integrity of the controlled system

Guyed tower: comparison of integrity profiles

Imperfect case ($\Omega = 0.505$, $\lambda = 0.7$, $u_{10} = 1°$ and $\xi = 0.01$)

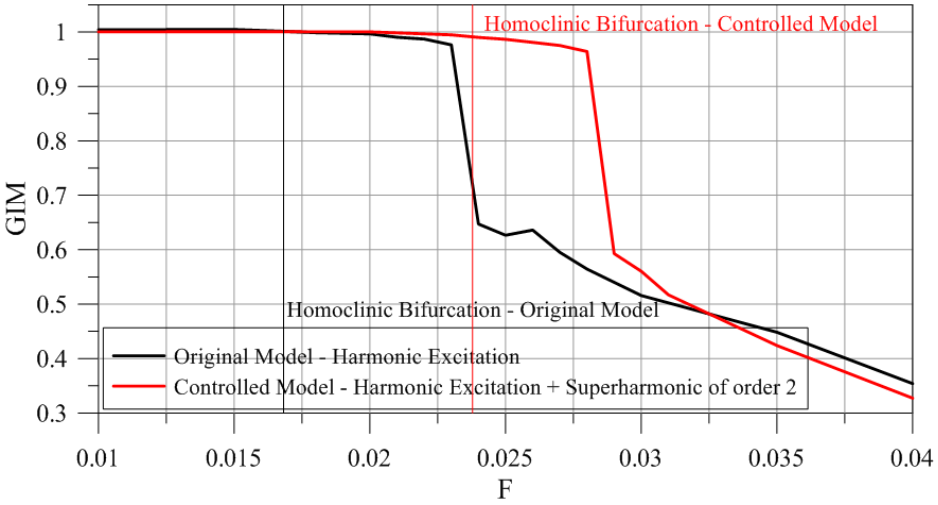

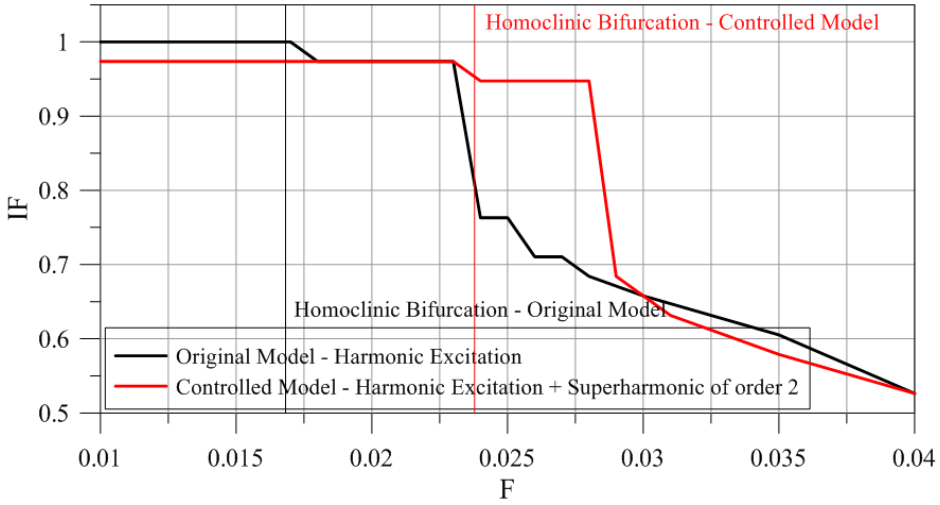

❖ Again, both GIM and IF show the increment of integrity of the controlled system

Guyed tower: perfect vs imperfect cases

❖ No major differences between perfect and imperfect cases (as instead occurs in the Augusti's model)

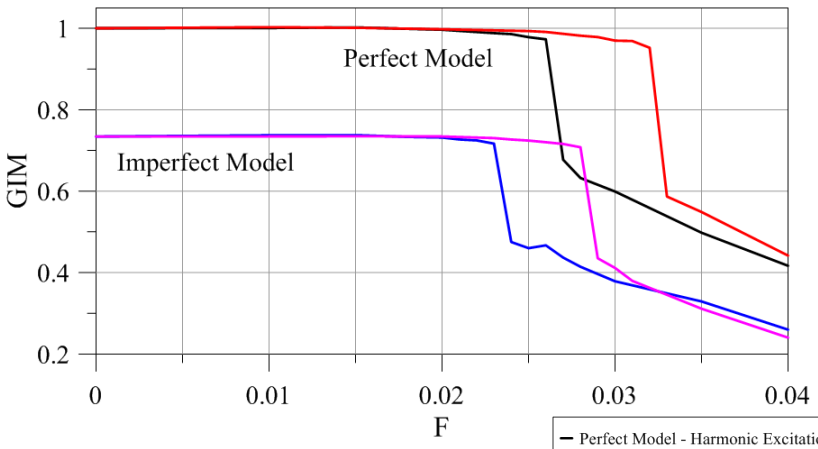

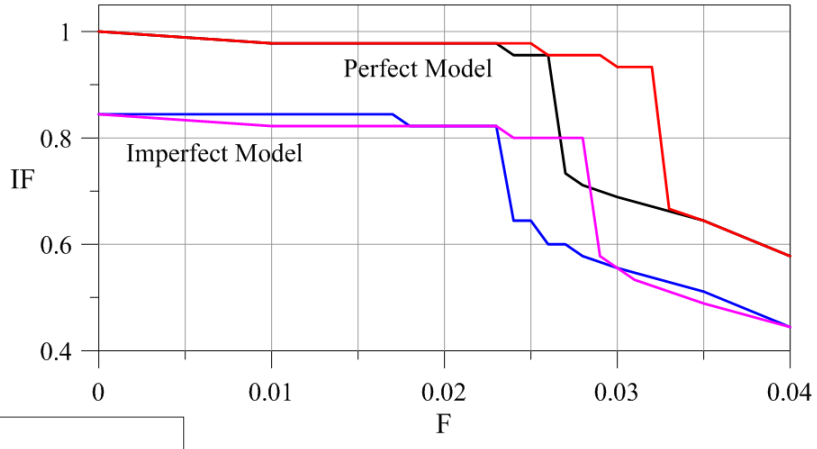

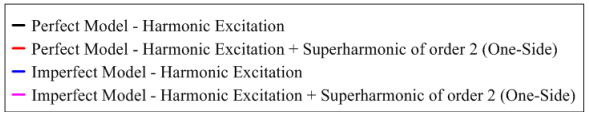

❖ Consequence of the fact that a homoclinic bifurcation is always involved (whereas in the Augusti's model there is a heteroclinic bifurcation in the perfect case and a homoclinic bifurcation in the imperfect case)

Contents

1. Integrity of in-well dynamics (Helmholtz, Duffing, Rigid block, MEMS, Augusti's model, Guyed Tower)
2. **Robustness/Integrity of competing (in-in/in-out) attractors** (Duffing, Parametrically excited pendulum, Parametrically excited cylindrical shell) → dynamical integrity only, no control

Duffing: competing non-resonant/resonant attractors (1)

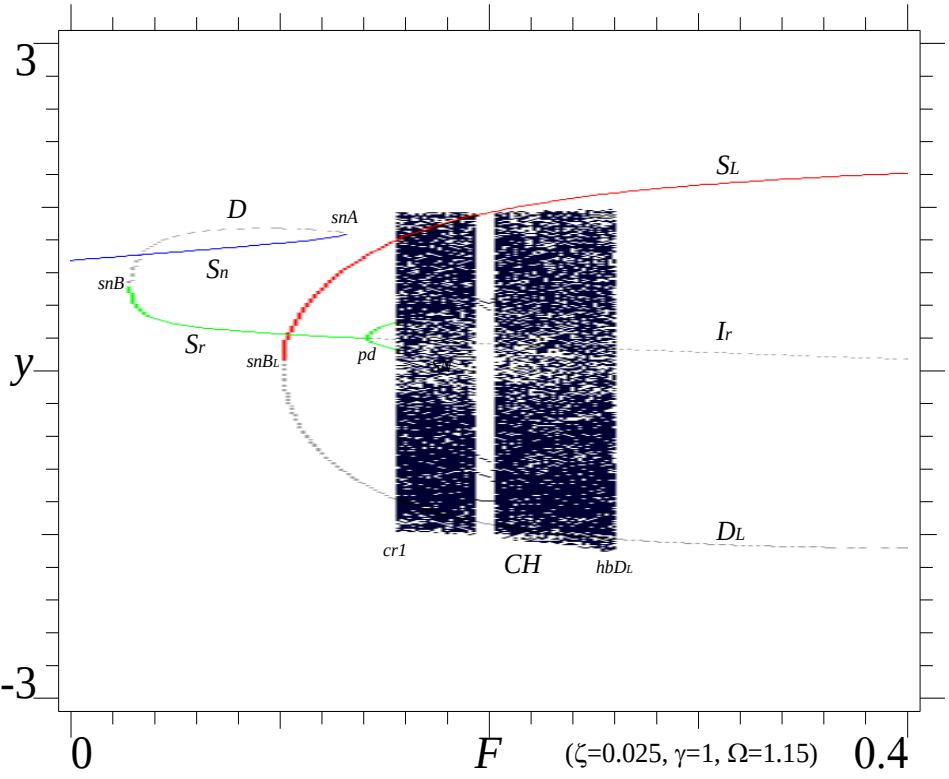

competing basins for increasing excitation amplitude:

a) only non-resonant attractor

b) onset of resonant attractor (at snB): sudden fall down of S_n vs new born S_r

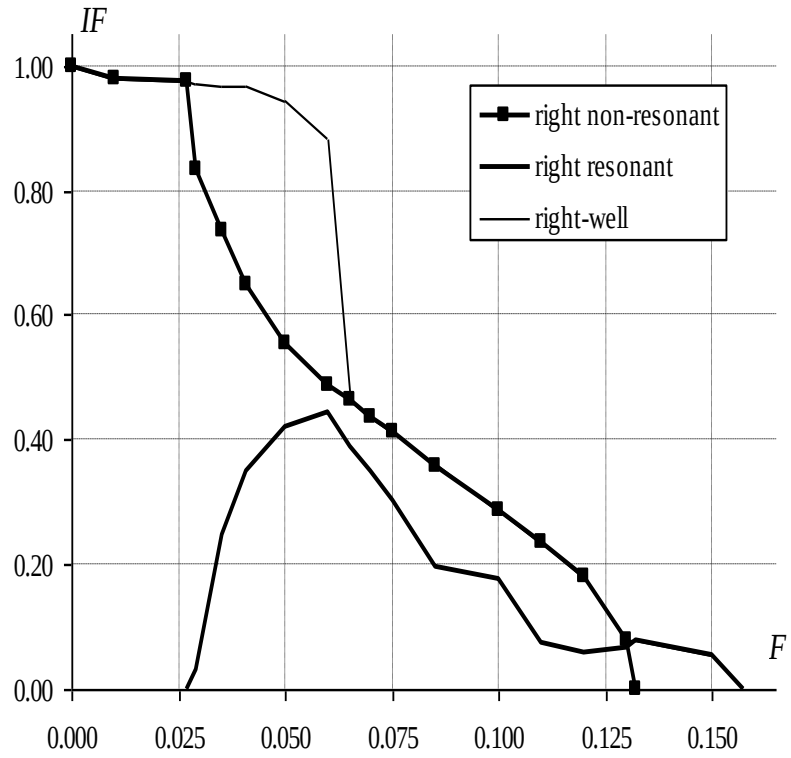

a) F = 0.027

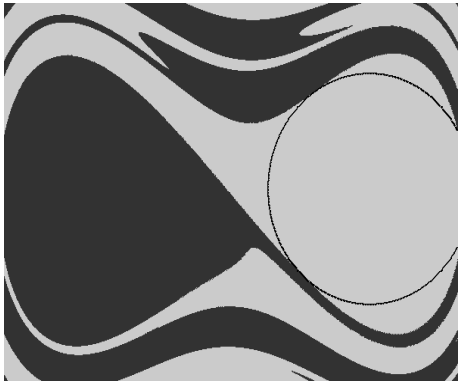

b) F = 0.029

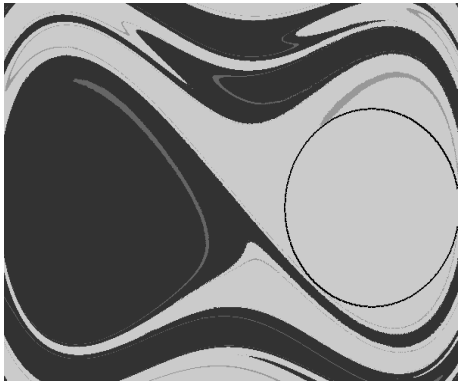

Duffing: competing non-resonant/resonant attractors (2)

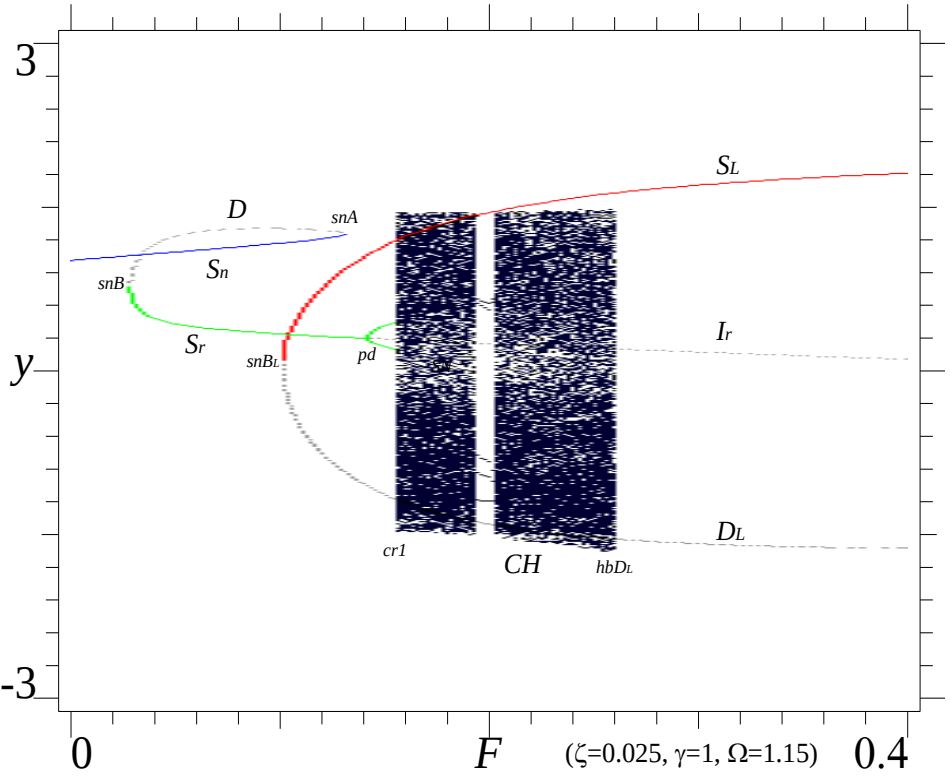

c) fractalization of left/right well basin boundaries (hb_h): no effect on compact basins

d) maximum basin of S_r

c) *F* = 0.041

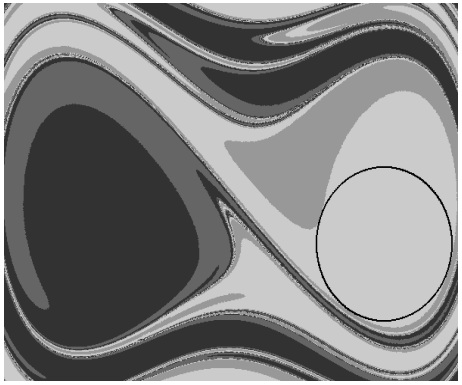

d) *F* = 0.060

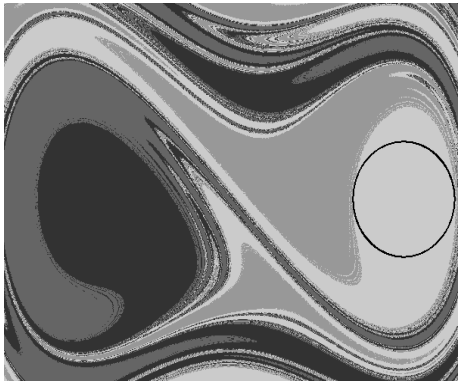

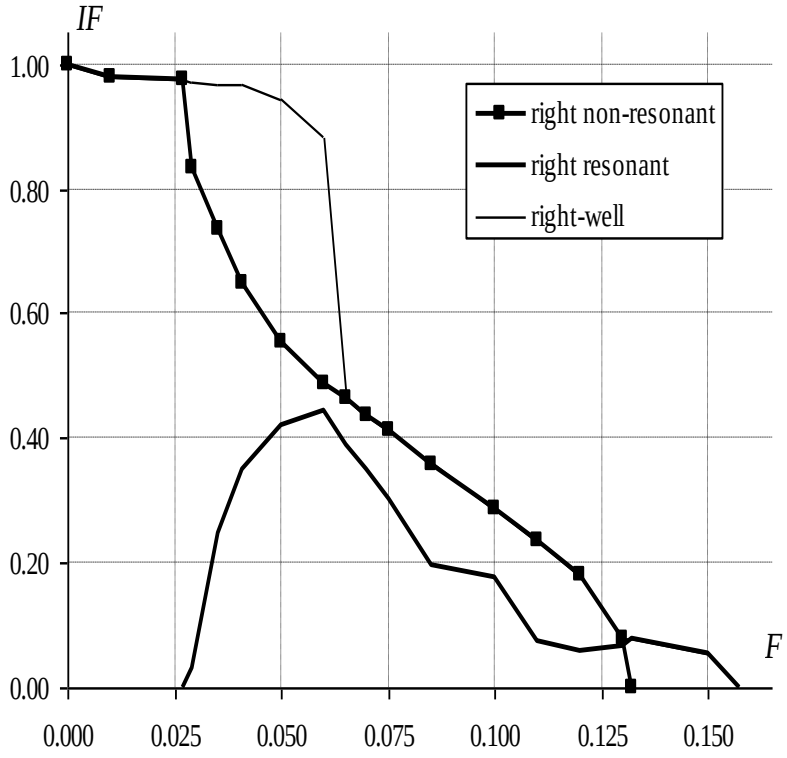

Duffing: competing non-resonant/resonant attractors (3)

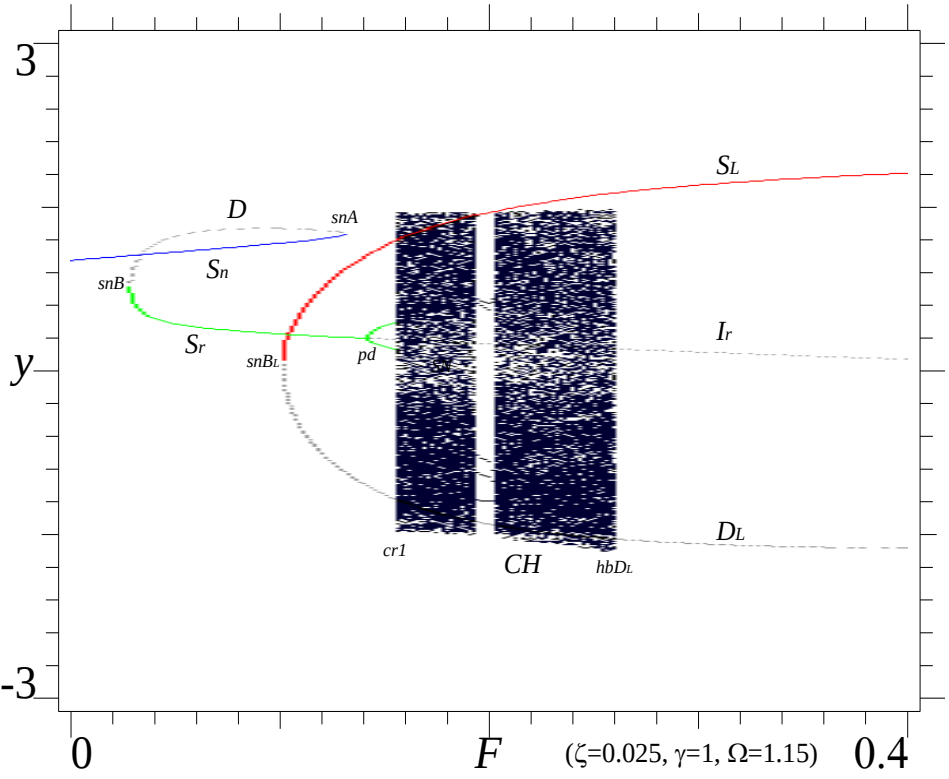

e) penetration of fractal tongues inside S_r basin

smoothly decreasing profiles till

f) near disappearance of S_n (at snA) and residual integrity of S_r

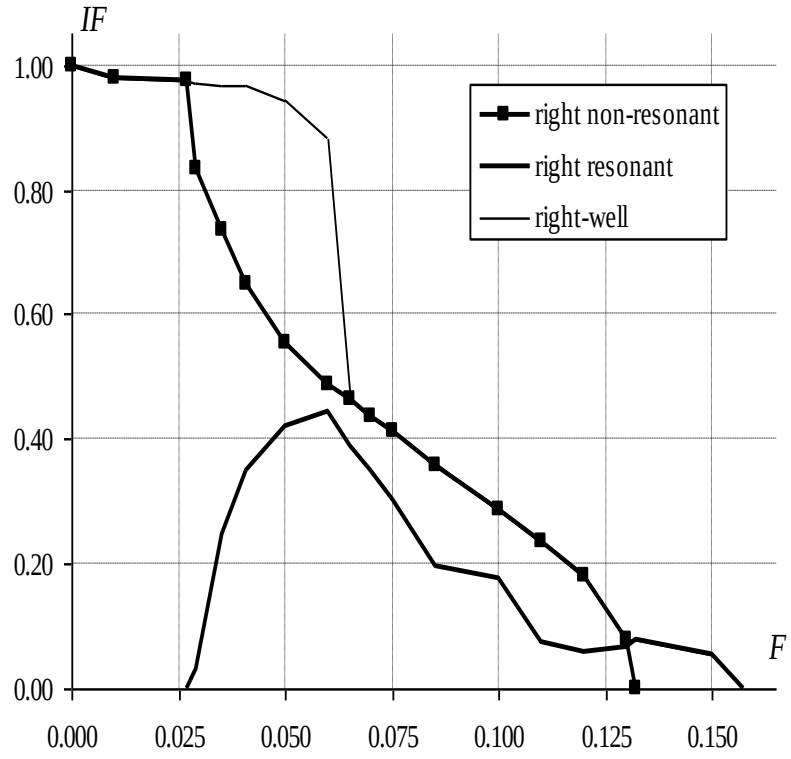

e) *F* = 0.065

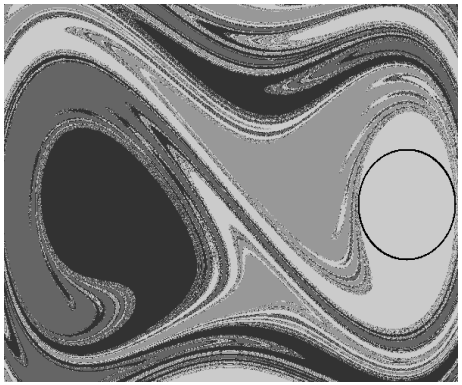

f) *F* = 0.130

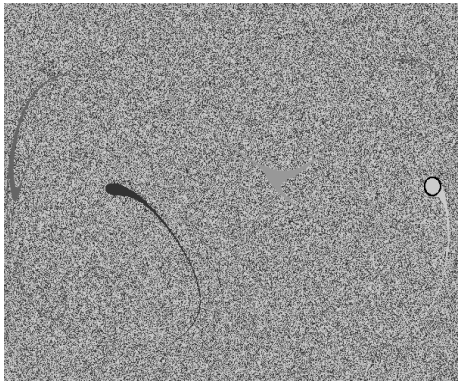

The parametrically excited mathematical pendulum

$$\ddot{x} + 0.1\dot{x} + [1 + p\cos(2t)]\sin(x) = 0$$

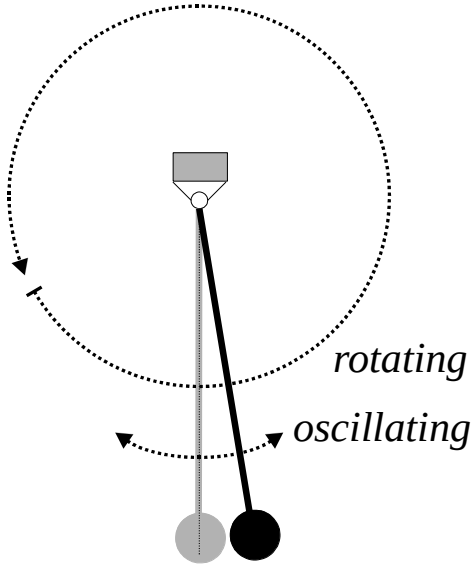

- "an antique but evergreen physical model" [Butikov]
- benchmark for main features of robustness and dynamical integrity of competing attractors
- permits a cross-study of in-well attractors (oscillations) and out-of-well attractors (rotations)
- has been recently shown to be of interest for practical applications [Xu et al., 2007]

Pendulum: bifurcation diagram and main events

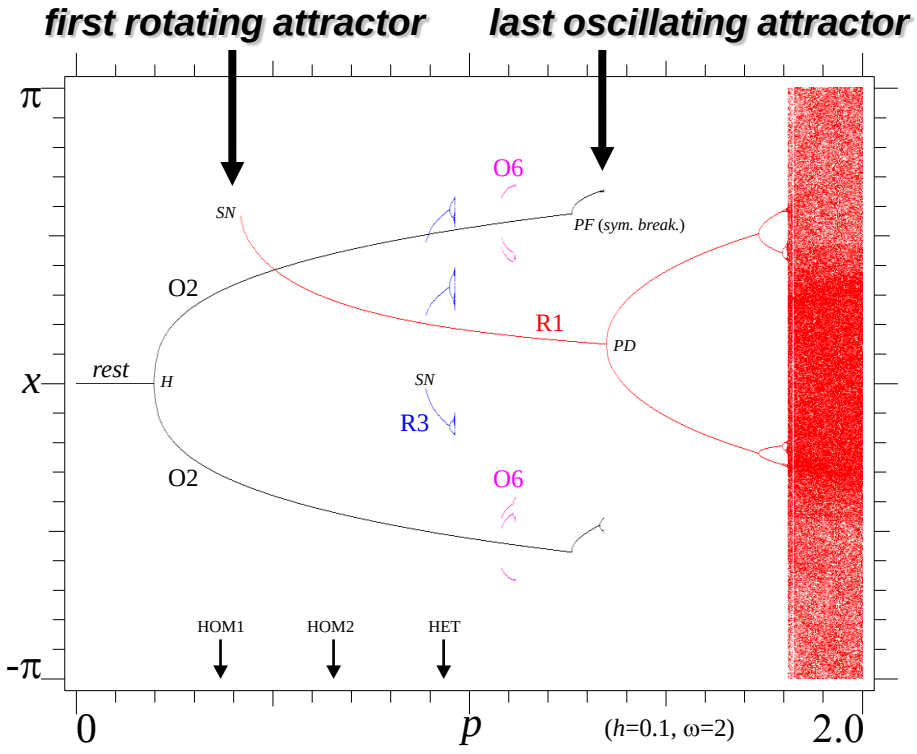

p	event	comment
0.196	H	the rest position loses stability. O2 appears
0.367	HOM1	homoclinic bifurcation of HS
0.418	SN	R1 appear through a SN bifurcation
0.655	HOM2	homoclinic bifurcation of DR1
0.888	SN	R3 appear through a SN bifurcation
0.935	HET	heteroclinic bifurcation of DR1 and Ir
0.948	PD	R3 undergo a PD bifurcation followed by a PD cascade
0.961	CR	the PD cascade of R3 ends by a CR. R3 disappear
1.082	SN	O6 appears through a SN bifurcation
1.111	PF	O6 undergoes a PF bifurcation, and two oscillating solutions of period 6, still named O6, appear
1.116	PD	O6 undergo a PD bifurcation followed by a PD cascade
1.118	CR	the PD cascade of O6 ends by a CR. O6 disappear
1.260	PF	O2 undergoes a PF bifurcation, and two oscillating solutions of period 2, still named O2, appear
1.332	PD	O2 undergo a PD bifurcation followed by a PD cascade
1.342	CR	the PD cascade of O2 ends by a CR. O2 disappear
1.349	PD	R1 undergo a PD bifurcation followed by a PD cascade
1.809	CR	the PD cascade of R1 ends by a CR. R1 disappear, and tumbling chaos becomes the unique attractor

attractors

O2	main oscillating solution of period 2
R1	main rotating solutions of period 1
R3	secondary rotating solutions of period 3
O6	secondary oscillating solution of period 6

main saddles

HS	hilltop saddles
DR1	direct saddles born at the SN bifurcation where R1 appear
IR1	inverse saddles after the PD bifurcation of R1
Ir	inverse saddle replacing the rest position at the H bifurcation

bifurcations

SN, PD	saddle-node, period-doubling
PF, H	pitchfork (or symmetry breaking), Hopf
CR	crisis
HOM/HET	homoclinic/heteroclinic

- four main competing attractors (O2, R1, O6, R3)
- ω=2 (parametric resonance)

Pendulum: integrity profiles at parametric res., ω=2

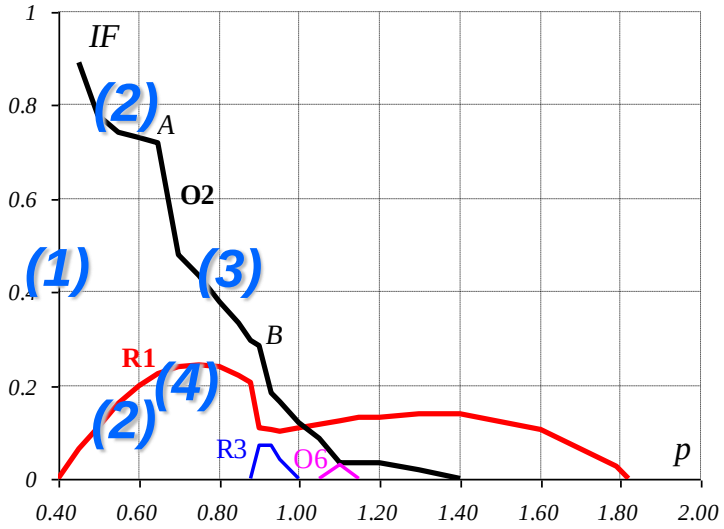

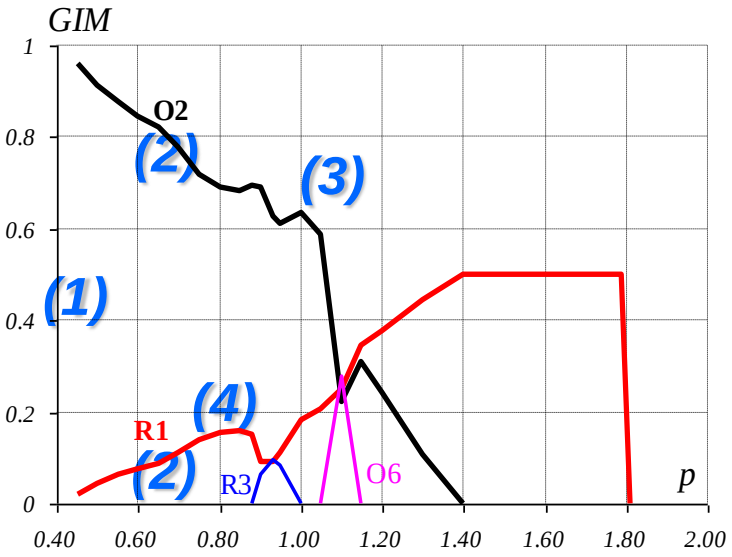

(1) starts when R1 are born by a SN

(2) R1 basins grow up against the O2 basin. This is described by IF and GIM, to a different extent

(3) both integrity curves of O2 have the classical "Dover cliff" behaviour

(4) IF and GIM integrity curves of R1 have a different qualitative behaviour

Pendulum: sudden falls

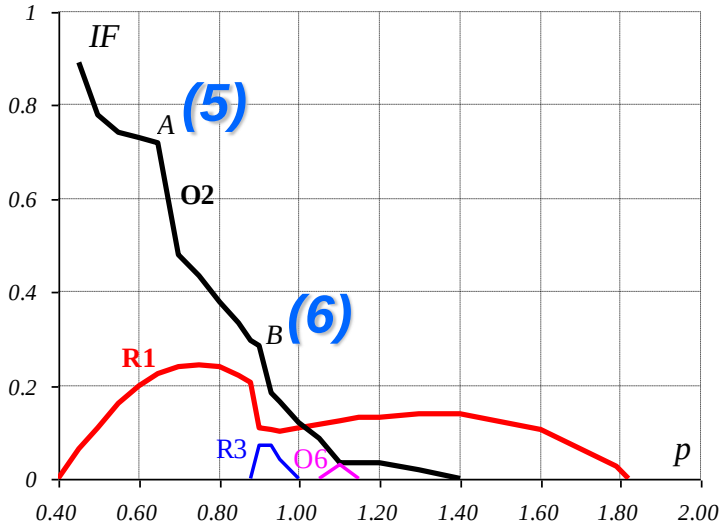

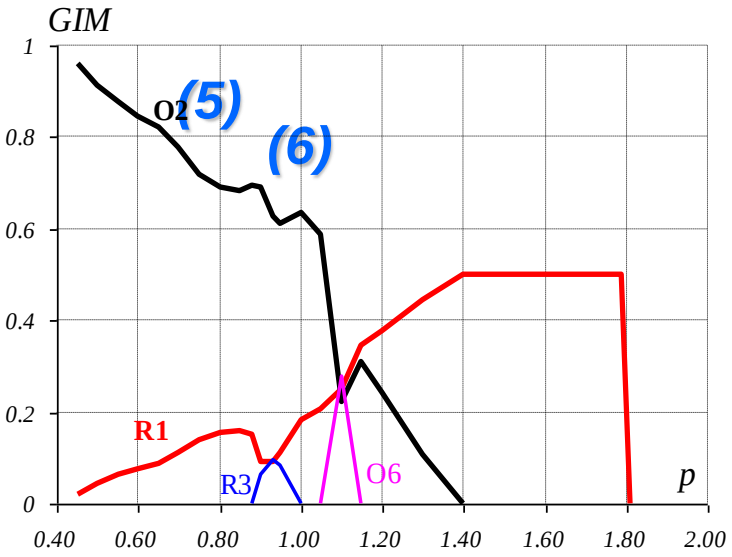

(5) sharp fall due to the homoclinic bifurcation of DR1: evidenced by IF but not by GIM

(6) sharp fall due to the het. bif. of DR1 and Ir: drastic reduction of the compact core of O2 basin clearly revealed by IF. With GIM this event is hardly recognizable (somehow hidden by the almost simultaneous appearance of R3)

Pendulum: final part of the erosion

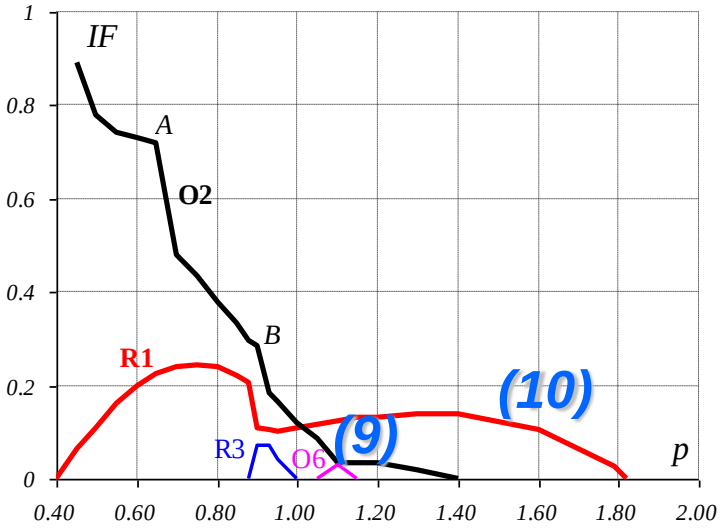

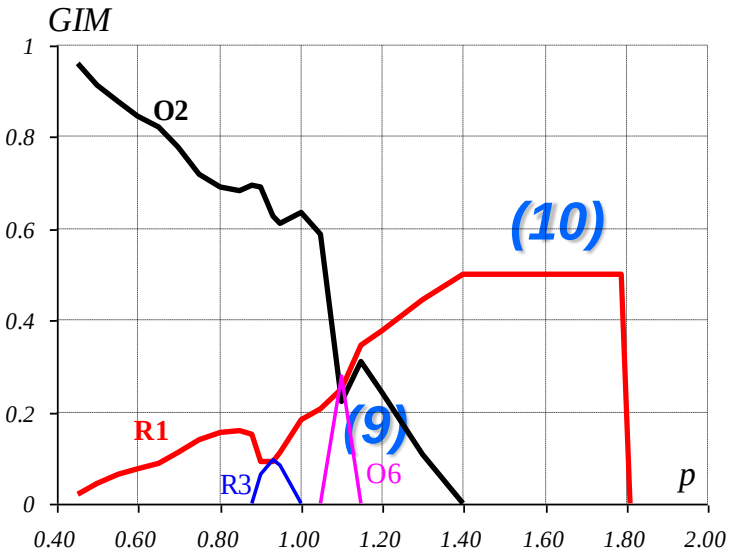

(9) O6 suddenly disappears, and O2 recovers a residual integrity by increasing the GIM and by keeping the IF constant

(10) no further special events up to the end of the integrity profiles
(by the BC of the respective attractors)

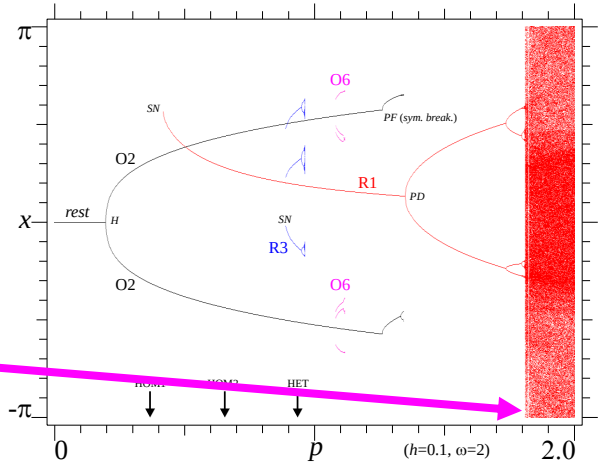

Pendulum: oscillating solutions

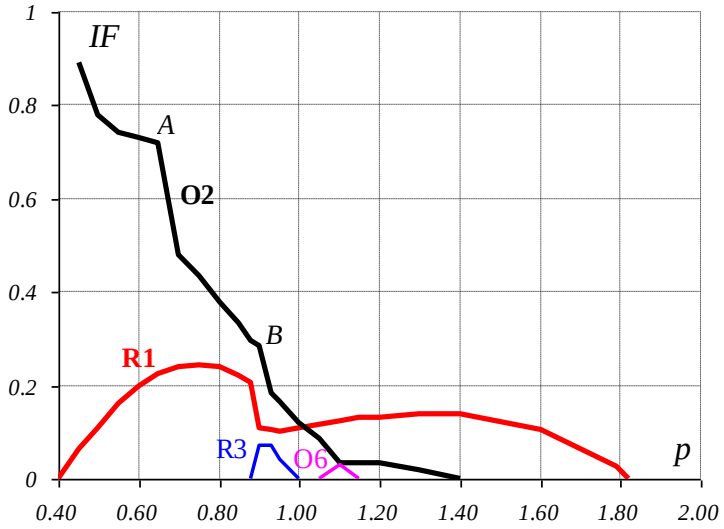

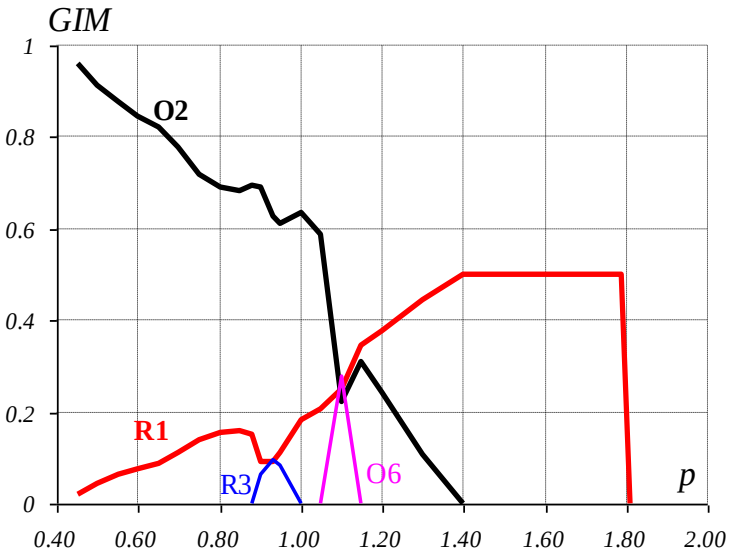

- IF and GIM erosion profiles of O2 are qualitatively similar. Differences in the final part: GIM→0 rapidly, IF →0 slowly
- GIM>>IF in the final part, thus GIM overestimates integrity of O2, which is residual

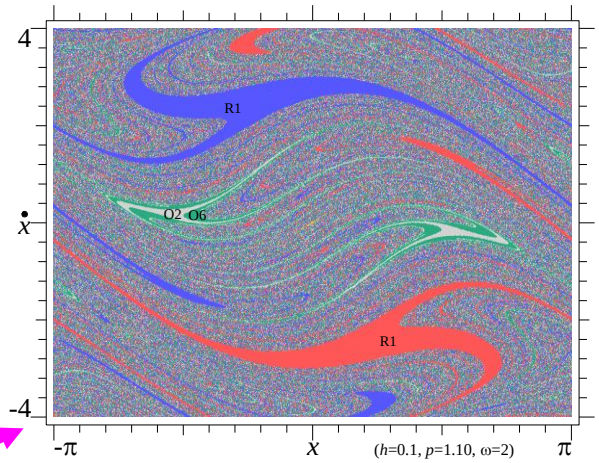

Pendulum: rotating solutions (1)

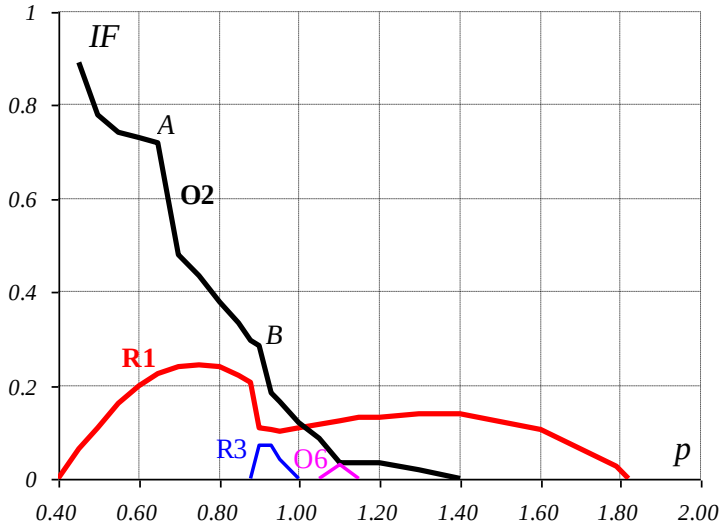

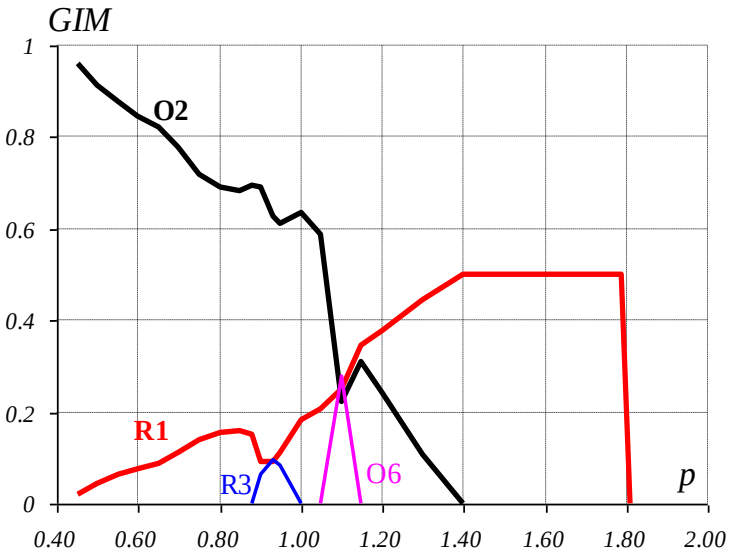

- R1 change ‘status’ for growing p. Initially they erode other (passive) attractors. Then, they are eroded by the secondary attractors, and finally they disappear by a reciprocal (self-) erosion

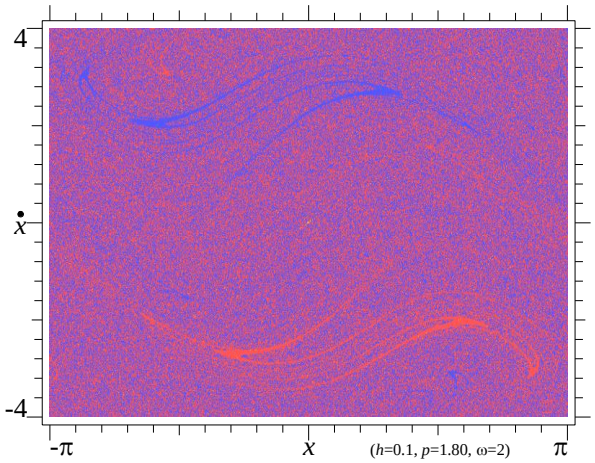

Pendulum: rotating solutions (2)

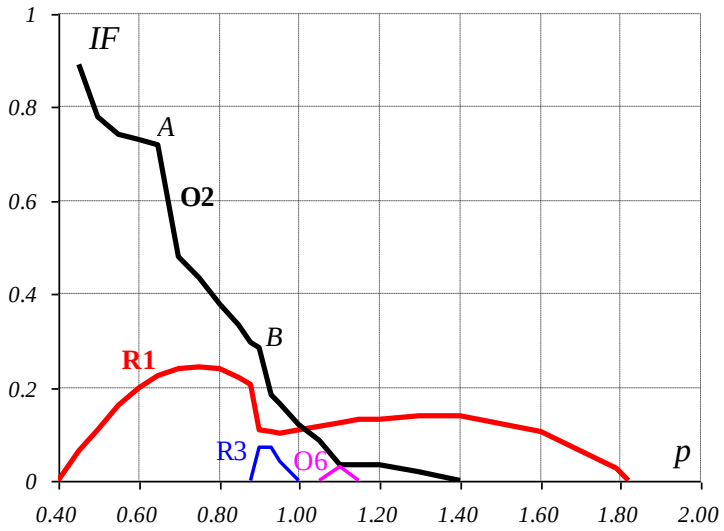

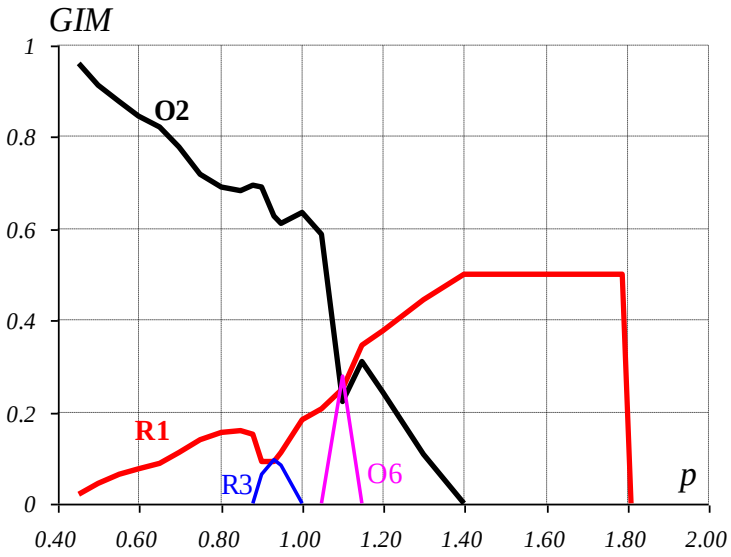

- differences between the IF and the GIM of R1 are much more marked than those of O2
- GIM is (almost monotonically) increasing up to 0.5
- IF initially increases, reaches a maximum, starts a dull decrement, undergoes a sudden falls due to R3, slightly increases and then slowly decreases again up to the end

Pendulum: attractor robustness and basin integrity

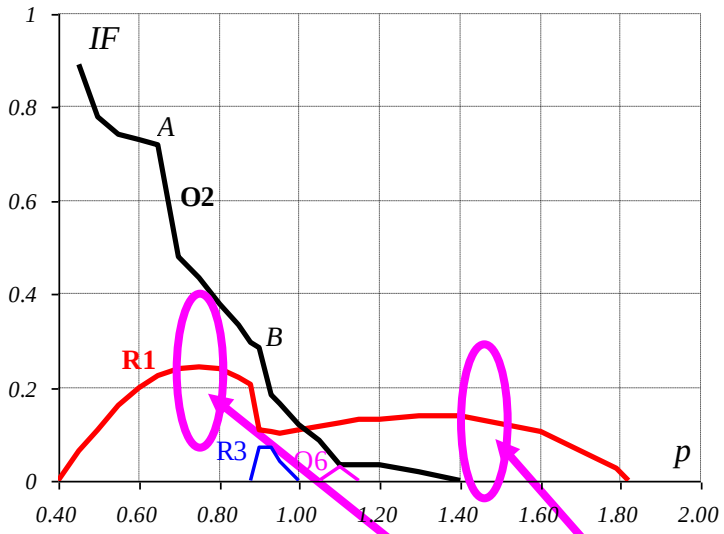

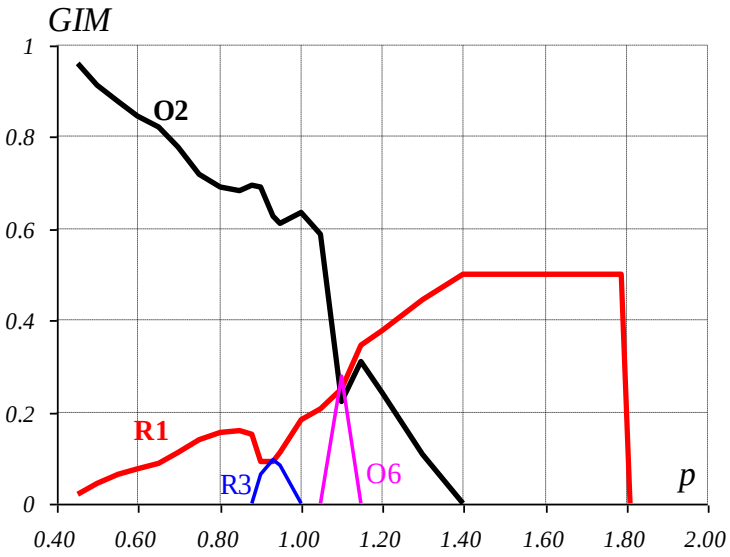

- qualitative difference of IF and GIM: GIM is basically also a measure of attractor robustness, whereas IF is a measure of basin integrity, of major interest for safe design
- sharp (O2) vs flat (R1) IF profiles
- optimal operating conditions for R1

Parametrically excited cylindrical shell (2-dof model)

$$\ddot{\zeta}_{11}+0.150761\dot{\zeta}_{11}+1.043914\zeta_{11}+9.274215\zeta_{11}\zeta_{02}-1.040775\Gamma_1\cos(\Omega\tau)\zeta_{11}$$
$$-1.043914\Gamma_0\zeta_{11}+0.274896\zeta_{11}^3+0.188199\zeta_{11}\zeta_{02}^2=0$$

$$\ddot{\zeta}_{02}+0.02086\dot{\zeta}_{02}-4.16310\Gamma_0\zeta_{02}-4.16310\Gamma_1\cos(\Omega\tau)\zeta_{02}+69.756712\zeta_{02}$$
$$+2.318554\zeta_{02}^2+0.094099\zeta_{11}^2\zeta_{02}=0$$

ζ_{11}, ζ_{02} basic, axisymm. mode with twice number of half waves in axial direction

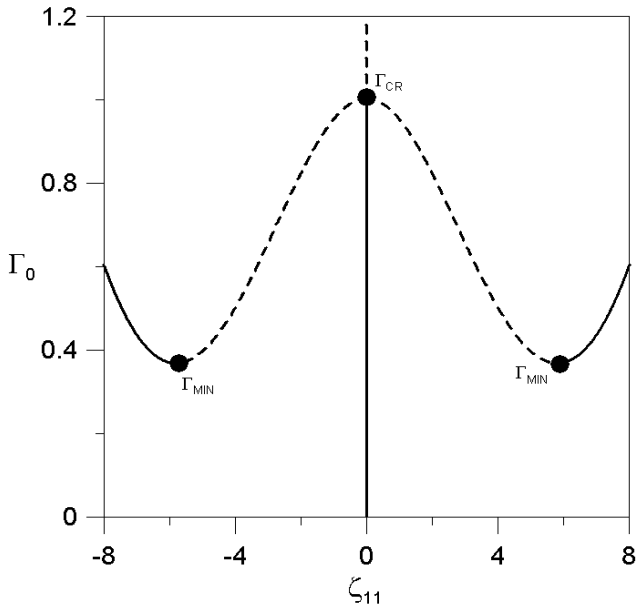

post-buckling response path
(Γ_0 , static load)

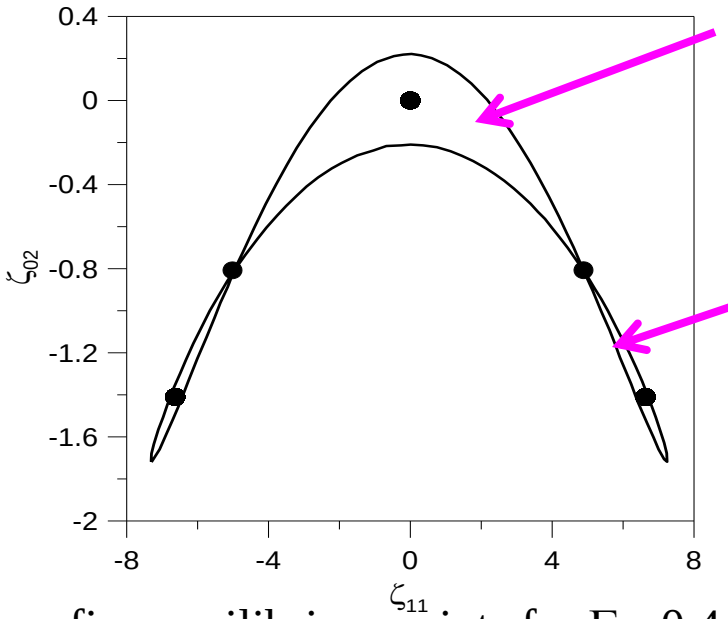

pre-buckling potential well

two post-buckling wells

five equilibrium points for Γ_0=0.4
(two heteroclinic and two homoclinic orbits)

Shell, sub-critical scenario: bifurcation diagram

increasing axial load amplitude Γ_1 in the main parametric instability region

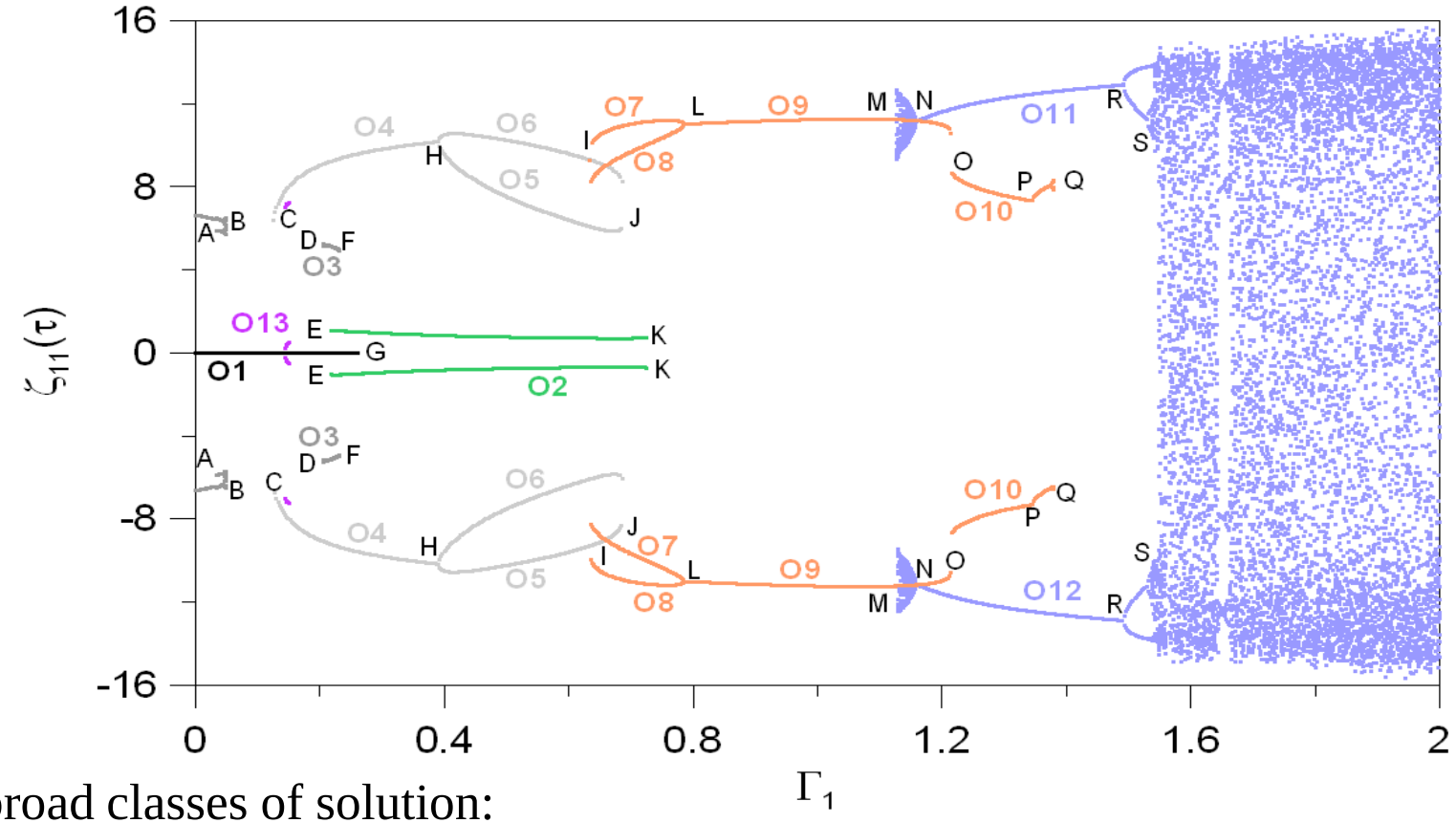

five different broad classes of solution:

(1) trivial pre-buckling,

(2) non-trivial 2T within the pre-buckling well,

(3) small amplitude vibrations within each of the post-buckling wells,

(4) medium amplitude cross-well,

(5) very large-amplitude cross-well period three, robust in the range

Shell, sub-critical: attractor-basin portrait (1)

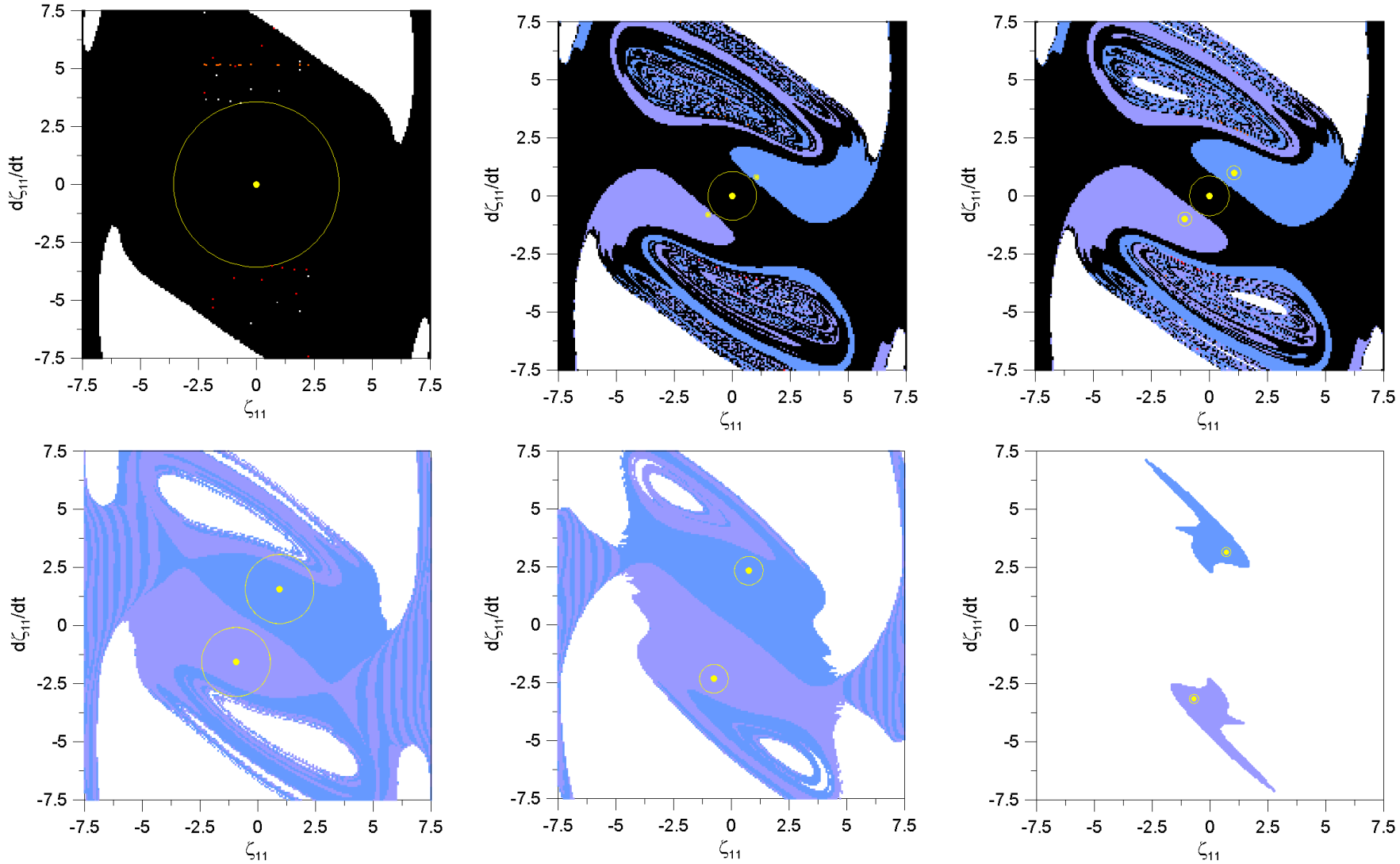

cross-sections of 4D basins of attraction: in-well pre-buckling attractors

Black: trivial. Light and dark blue: period two. White: escape

Shell, sub-critical: attractor-basin portrait (2)

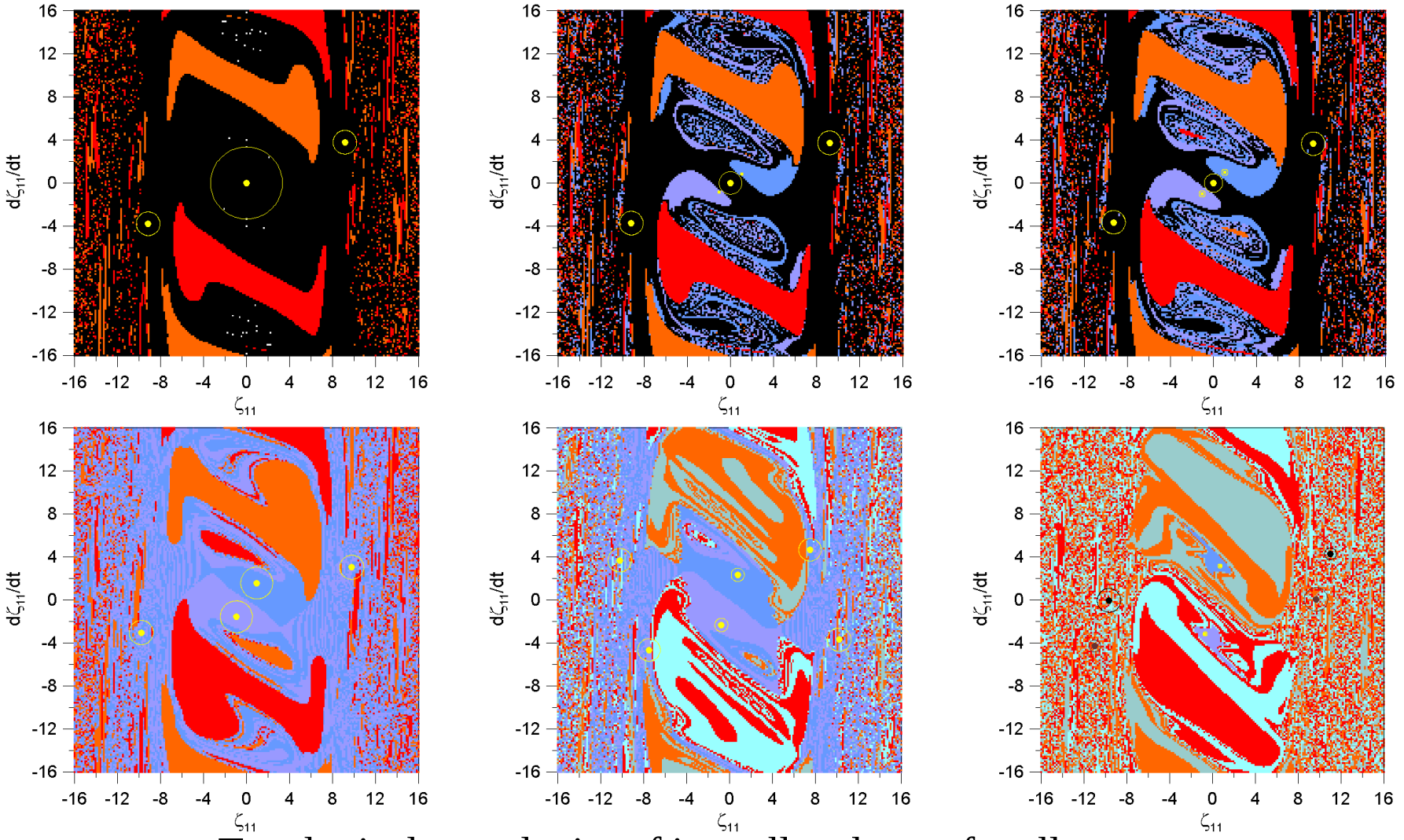

Topological complexity of in-well and out-of-well attractors.

Remark: Being basins of attraction in a 4D hyper-volume, it is not easy to detect touching of the hypersphere with the nearest competing basin

Shell, sub-critical scenario: dynamic integrity

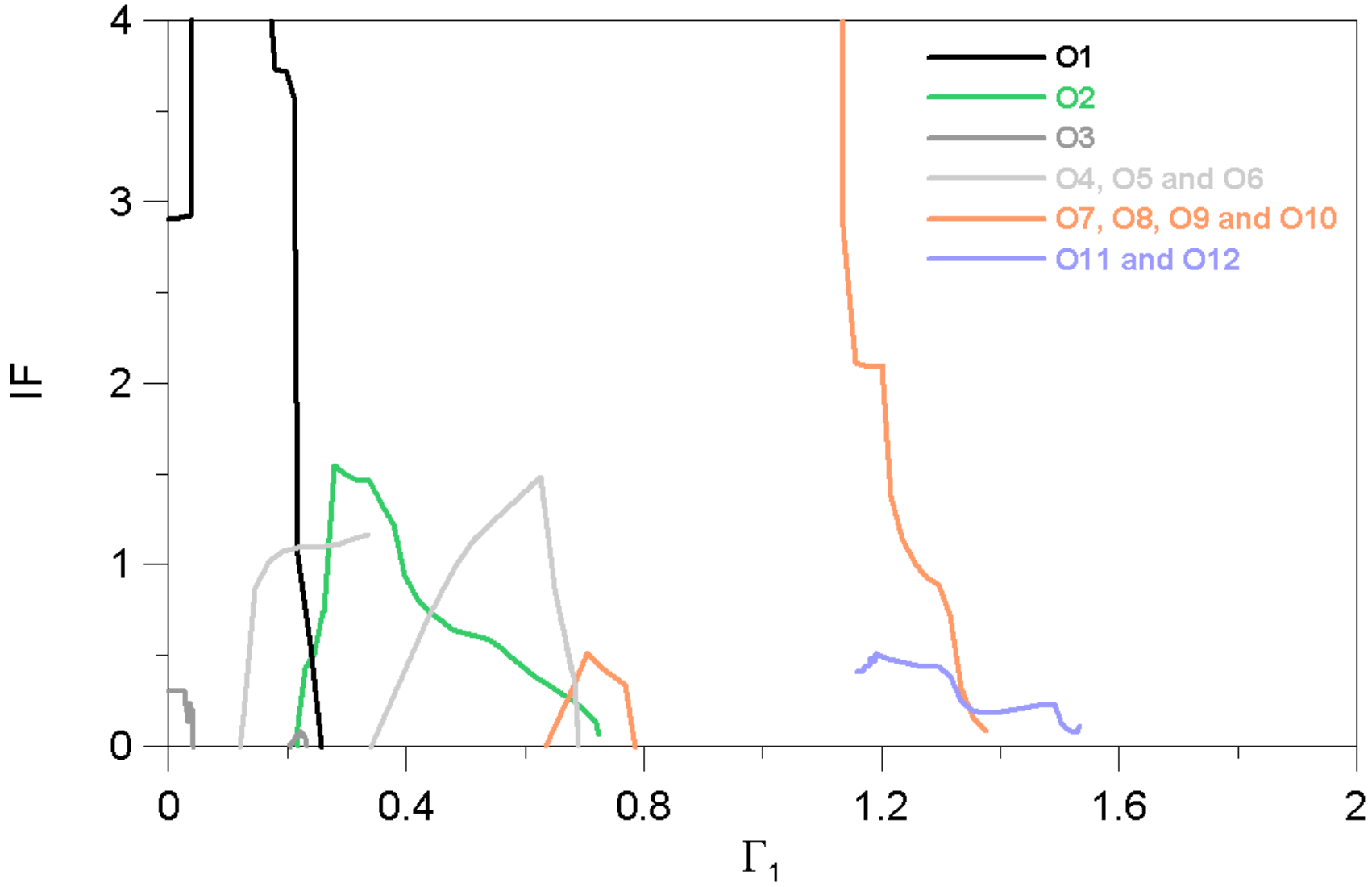

erosion profiles of competing attractors